FUNCTIONAL CHARACTERIZATION OF KPNA7, A NEW MEMBER OF CLASSICAL NUCLEAR LOCALIZATION SIGNAL RECEPTOR FAMILY

（新規古典的核局在化シグナル受容体ファミリーKPNA7 の機能解析）

Chihiro Kimoto[1,2]

Advising teacher : Yoshihiro Yoneda[1,3]

[1]Biomolecular Dynamics Laboratory, Department of Frontier Bioscience, Graduate School of Frontier Bioscience, Osaka University, 1-3 Yamada-oka, Suita, Osaka 565-0871, Japan.

[2]Laboratory of Nuclear Transport Dynamics, National Institute of Biomedical Innovation, 7-6-8 Saito-Asagi, Ibaraki, Osaka 675-0085, Japan.

[3]National Institute of Biomedical Innovation, 7-6-8 Saito-Asagi, Ibaraki, Osaka 675-0085, Japan.

Finished the doctor’s course in March 2015

ABSTRACT

Karyopherin alpha 7 (KPNA7) has recently been identified as a new member of the importin α family, which consists of classical nuclear localization signal (cNLS) receptor proteins, based on its amino acid similarity with and binding ability to importin β1. However, it remains unclear whether KPNA7 is involved in the nuclear transport of proteins. In this study, using an *in vitro* transport assay in digitonin-permeabilized cells, I demonstrated that bacterially produced, purified KPNA7 can transport SV40 T antigen cNLS-containing cargo into the nucleus of HeLa cells in conjunction with importin β1. Using pull-down assay and mass spectrometry analysis of KPNA7 stably expressed in HEK293 cells, I identified 179 putative KPNA7-binding proteins, 62 of which also bound to KPNA2, the importin α family member most similar to KPNA7. Among the 117 KPNA7 binding candidates, I focused further study on DDB2 and demonstrated that KPNA7 transports the protein into the nucleus, indicating that it indeed acts as an NLS receptor. In addition, KPNA7 was found to heterodimerize with other importin α family members such as KPNA3 and KPNA4. Furthermore, ectopic expression of KPNA7 in HeLa cells induced nuclear co-localization of these KPNAs, indicating that KPNA7 negatively regulates the nuclear protein transport. Based on these results, I hypothesize that KPNA7 plays a dual role in nuclear protein import: it functions not only as a nuclear transport factor, but also

as a nuclear transport regulator through the control of the subcellular localization of other importin α members.

TABLE OF CONTENTS

ABBREVIATIONS

Apoptosis-inducing factor 1, mitochondrial: AIFM1,
Bovine serum albumin: BSA,
Cyclin B1: CCNB,
Cytoplasmic FMR1-interactiong protein 2: CYFIP2,
DNA damage-binding protein 2: DDB2,
Fanconi anemia group I protein: FANCI,
Glutathione Sepharose 4B slurry: GSH beads,
Importin subunit α4: KPNA3,
Lysine-specific histone demethylase 1: KDM1A,
Moesin: MSN,
Nuclear localization signal: NLS,
Nuclear pore complex: NPC,
Polyacrylamide gel electrophoresis: PAGE,
Protein pelota homolog: PELO,
Rab3 GTPase-activating protein non-catalytic subunit: RAB3GAP2,
Regulatory-associated protein of mTOR: RPTOR,
Sortilin: SORT1,
Structural maintenance of chromosomes protein 1A: SMC1A,
Telomere length regulation protein TEL2 homolog: TELO2

BACKGROUND

In eukaryotic cells, the nucleus is separated from the cytoplasm by a nuclear membrane, which is a double lipid bilayer; therefore, the nucleocytoplasmic transport must occur through the nuclear pore complex (NPCs) embedded in the nuclear membrane (Hoelz et al, 2011). The NPCs consist of multiple copies of approximately 30 distinct proteins called nucleoporins in both yeast and mammals (Cronshaw et al., 2002; Rout et al, 2000; Wente & Rout, 2010). Macromolecules larger than ~40 kDa such as proteins and mRNAs can be selectively transported into and out of the nucleus in a signal-dependent manner, while molecules smaller than ~40kDa such as ions and small proteins can pass through the NPC by passive diffusion (Wente & Rout, 2010). Active protein transport through the NPCs typically involves a transporter molecule that recognizes a transport signal on the cargoes, a nuclear localization signal (NLS) for import to the nucleus or a nuclear export signal (NES) for export from the nucleus (Sorokin et al, 2007).

The classical NLS (cNLS), consisting of basic amino acid cluster(s), is recognized by and binds to a transport factor importin α that forms a trimeric complex with importin β1, which mediates the interaction of the complex with the nuclear pore (Madrid & Weis, 2006). Importin α consists of an N-terminal importin β-binding (IBB) domain and 10 armadillo (ARM) repeats which have 2 cNLS binding pockets called a major NLS-binding site located between the 2nd

and 4th ARM repeats and a minor NLS-binding site at the 6th and 8th ARM repeats (Fontes et al, 2000; Goldfarb et al, 2004). The accessibility of the NLS-binding sites is regulated by an autoinhibitory mechanism mediated by the IBB domain (Kobe, 1999). Crystallography analysis revealed that the SV40 large T antigen NLS (SV40T-NLS: PKKKRKV^{132}) and nucleoplasmin NLS (NP-NLS: KRPAATKKAGQAKKKK^{171}) bind to the major binding and to both the major and minor binding site, respectively (Fontes et al, 2000). After the cNLS substrate-importin α-importin β1 trimeric complex enters the nucleus through the NPC, the cargo proteins are released from importin α by binding of the GTP-bound small GTPase Ran (RanGTP) to importin β1. Importin α is exported from the nucleus by the cellular apoptosis susceptibility (CAS) gene product in conjunction with RanGTP, and importin β1 leaves the nucleus in a complex with RanGTP (Sorokin et al, 2007).

INTRODUCTION

Active nuclear transport plays central roles in many biological processes such as the regulation of intracellular signal transduction. Nuclear proteins that are synthesized in the cytoplasm are actively transported into the nucleus by transport factors. The general name for the class of transport factors that carry cargo between the nucleus and cytoplasm is karyopherins. These are classified into two distinct groups: importins, which mediate protein transport into the nucleus, and exportins, which carry proteins out of the nucleus. Importins are the most widely studied transport factors and are further categorized into importin α and importin β; importin α serves as an adaptor by connecting a cargo protein to importin β1.

Importin α, also known as karyopherin α, is recognized as a cNLS receptor molecule, and seven importin αs have been identified in human and six in mouse, which were classified into three subfamilies based on their amino acid sequence similarity (Goldfarb et al, 2004; Miyamoto et al, 2012). For historical reasons centering on different usage of the terms "importin" and "karyopherin," the importin α gene nomenclature is complicated and the two terms "importin α" and "karyopherin α" have been used interchangeably. Moreover, differences in the number of importin α genes between human and mouse have led to homologs having different names, which has added to the confusion; for example, human importin α5 (also referred to as KPNA1) is termed importin α1 (Kpna1) in mouse.

Table 1 provides the gene symbols for importin α (karyopherin α) in both human and mouse. In the present study, I used the term "KPNA" instead of "importin α," because the KPNA homologs have the same name number in human and mouse. The KPNA genes can be classified into three subfamilies based on their sequence; a subfamily consisting of KPNA2 and KPNA7, one consisting of KPNA3 and KPNA4, and one consisting of KPNA1, KPNA5, and KPNA6. The various members are differentially expressed in tissues and cell types and display cargo specificity (Kohler et al, 1997; Kohler et al, 1999; Miyamoto et al, 1997; Tsuji et al, 1997). Recently, it has been reported that KPNAs are implicated in various biological processes in Metazoa. For example, KPNA1 was shown to play a critical role in the development of mammalian female reproductive organs (Moriyama et al, 2011). KPNA2 is involved in the cell fate decisions of mouse embryonic stem (ES) cells (Yasuhara et al, 2013). In addition, fruit fly (*Drosophila melanogaster*) mutants lacking KPNA1 or KPNA2 show deleterious gametogenesis defects (Ratan et al, 2008, Mason et al, 2002). Furthermore, fruit flies in which the KPNA3 gene is mutated die around the first larval molt (Mason et al, 2003).

KPNA7 is the most recently identified KPNA family member (Tejomurtula et al, 2009). KPNA7 amino acid sequences are conserved among human, mouse, bovine, and porcine species (Tejomurtula et al, 2009; Hu et al, 2010; Kelley et al, 2010; Park et al, 2012). It has been reported that KPNA7 is expressed in mouse oocytes, zygotes, and two-cell stage embryos

Table 1. The nomenclature of importin (karyopherin) α-subtypes.

human/mouse	human	mouse
karyopherin α	importin α	imporitn α
KPNA1	*IMPα5*	*Impα1*
KPNA2	*IMPα1*	*Impα2*
KPNA3	*IMPα4*	*Impα3*
KPNA4	*IMPα3*	*Impα4*
KPNA5	*IMPα6*	*Non*
KPNA6	*IMPα7*	*Impα6*
KPNA7	*IMPα8*	*Impα8*

(Hu et al, 2010). In germinal vesicle stage oocytes, zygotes, and two-cell stage embryos, KPNA7 is localized in the nucleus, while in MII oocytes, it is localized in the spindle (Hu et al, 2010). KPNA7 knockout mouse showed embryonic lethality and preimplantation developmental abnormalities (Hu et al, 2010). Interestingly, it has recently been demonstrated that KPNA7 can bind to importin β1 via the IBB domain, but not to the SV40T-NLS, a cNLS, which means that KPNA7 cannot function as a cNLS receptor (Kelley et al, 2010).

However, in this study, I demonstrated that KPNA7 actually does function as a cNLS receptor. In addition, because the amino acid similarity between KPNA7 and KPNA2 is rather low, I analyzed their specific cargo proteins. Proteomic analysis of the KPNA7- and KPNA2-binding proteins showed that the binding partners are significantly different, which indicates that KPNA7 and KPNA2 play different roles in the nuclear protein import. Furthermore, the data showed that KPNA7 is mainly localized in the nucleus where it binds to other KPNA members to form heterodimers, suggesting that KPNA7 functions as a negative regulator of nuclear protein import through the suppression of KPNA recycling.

MATERIALS AND METHODS

Plasmid construction

The sequences of all the primers used in this study are presented in Table 2. The full-length human KPNA7 (hKPNA7, 1,548 base pairs) cDNA was amplified from HeLa cells using the primers hKPNA7 Fwd and hKPNA7 Rev, and the PCR products were ligated into the *Bam*HI and *Xho*I sites of the pGEX6P1 vector (GE Healthcare, Tokyo, Japan) or ligated into the *Bgl*II and *Sal*I sites of the pEGFPC1 vector (Takara Bio, Shiga, Japan). The plasmids pGEX6P2-mouse KPNA2 (mKPNA2), pGEX2T-importin β1, pGEX6P1-Ran, pGEX6P1-NTF2, pGEX2T-SV40T-NLS-GFP, pGEX6P3/flag-hKPNA1, pGEX6P3/flag-hKPNA2, and pGEX6P3/flag-hKPNA4 were obtained as described previously (Sekimoto et al, 1997; Yasuhara et al, 2013; Yokoya et al, 1999). The plasmid pGEX6P3-mKPNA2ED was constructed from pGEX2T-mKPNA2ED, which has been described previously (Arjomand et al, 2014). The coding sequence of mKPNA2 including two point mutations at D192K and E396R was amplified using the primers mKPNA2 Fwd and mKPNA2 Rev, and inserted into the *Eco*RV site of pBluescript II KS(+) (Stratagene, California, USA). The PCR thermal cycles were as follows: 1 cycle of 2 min at 94 °C followed by 30 cycles of 10 sec at 98 °C, 30 sec at 61 °C, and 1 min at 68 °C. The product was inserted into *Eco*RI-*Xho*I-digested pGEX6P3 vector (GE Healthcare). To construct the hKPNA7ED (D186K/E386R) mutant, the PCR primers hKPNA7 D186K Fwd and hKPNA7

from185 Rev were used to create the D186K mutation by site-directed mutagenesis in the pBluescript-hKPNA7 cloning construct. Thermal cycles were as follows: 1 cycle of 2 min at 94 °C followed by 30 cycles of 10 sec at 98 °C and 2 min 20 sec at 68 °C. After the construct was digested with *Dpn*I (New England Biolabs Japan, Japan), the product was ligated with Ligation high Ver.2 (Toyobo, Japan) and T4 kinase (Toyobo). The PCR primers hKPNA7 E386R Fwd and hKPNA7 from385 Rev were used to introduce the mutation E386R using the pBluescript-hKPNA7(D186K) construct. Thermal cycles were as follows: 1 cycle of 2 min at 94 °C followed by 30 cycles of 10 sec at 98 °C and 2 min 20 sec at 68 °C. After digestion of the construct with *Dpn*I, the product was ligated with Ligation High ver.2 and T4 kinase. The mutations were confirmed by Sanger sequencing and the products were cloned into the *Bam*HI and *Xho*I sites of pGEX6P1.

To create the pcDNA5/FRT/3xFLAG expression construct, three tandem repeats of the FLAG oligonucleotide were inserted into the *Nhe*I and *Bam*HI sites of the pcDNA5/FRT vector (Life Technologies), and then the coding region of hKPNA7 or hKPNA2, which was amplified by PCR from pGEX6P3/flag-hRch1 (Sekimoto et al, 1997), was cloned into the *Bam*HI and *Xho*I sites of pcDNA5/FRT/3xFLAG expression vector.

Genes encoding putative importin α-binding proteins were amplified from cDNA of HeLa cells using primers indicated in Table 2, and then cloned into pENTR/D-TOPO cloning

kit (Invitrogen). The following putative importin α-binding proteins were cloned: moesin (MSN), sortilin (SORT1), isoform 2 of cytoplasmic FMR1-interactiong protein 2 (CYFIP2), structural maintenance of chromosomes protein 1A (SMC1A), isoform 1 of Rab3 GTPase-activating protein non-catalytic subunit (RAB3GAP), isoform 1 of regulatory-associated protein of mTOR (RPTOR), isoform 1 of apoptosis-inducing factor 1, mitochondrial (AIFM1), cyclin B1 (CCNB), isoform 1 of DNA damage-binding protein 2 (DDB2), isoform 3 of Fanconi anemia group I protein (FANCI), isoform 2 of lysine-specific histone demethylase 1 (KDM1A), importin subunit α4 (KPNA3), protein pelota homolog: (PELO), and telomere length regulation protein TEL2 homolog (TELO2). Thermal cycles were as follows: 1 cycle of 2 min at 94 °C followed by 40 cycles of 10 sec at 98 °C and 2 min 45 sec, 1 min 30 sec, 2 min 5 sec, or 2 min 50 sec at 68 °C, depending on the length of the PCR product. To transfer the candidate genes from the pENTR to the p3xHA-CMV destination vector, the Multisite Gateway cloning system (Invitrogen, Darmstadt, Germany) was used. To generate p3xHA-CMV, three tandem repeats of the hemagglutinin (HA) tag were inserted into *Nhe*I and *Bam*HI sites of pcDNA3.1Zeo(+) (Life Technologies). The Reading Frame Cassette of the Gateway Conversion System (Invitrogen) was inserted into the *Eco*RV site of p3xHA-CMV.

The DDB2 coding sequence was amplified from p3xHA/CMV-DDB2 using the primers CCC *Bam*HI DDB2 Fwd and GGG *Bam*HI C DDB2 Rev. Thermal cycles were as follows: 1

cycle of 2 min at 94 °C followed by 30 cycles of 10 sec at 98 °C and 44 sec at 68 °C. The PCR products were digested with *Bam*HI and *Xho*I, and then cloned into the pGEX6P2/hGFP vector, which is an expression vector of glutathione S-transferase (GST)-fused green fluorescent protein (GFP).

Purification of recombinant proteins

Bacterially expressed recombinant proteins fused to GST were purified as described previously (Miyamoto et al, 2013; Miyamoto et al, 1997). Cleavage of the GST tag to yield cleaved fusion proteins hKPNA7, mKPNA2, Ran, and NTF2 was done using PreScission protease (10 U/mg of fusion protein, GE Healthcare) in cleavage buffer (50 mM Tris-HCl (pH 7.0), 150 mM NaCl, 1 mM EDTA 3Na (Nacalai Tesque, Kyoto, Japan), 1 mM DTT (Nacalai Tesque)) at 4 °C overnight. Importin β1 was cleaved with thrombin protease (10 U/mg of fusion protein, Sigma-Aldrich, Germany) in cleavage buffer. To create the nucleotides bound form of Ran, cleaved Ran was incubated with 25 mM EDTA 3Na and 2 mM GDP (Sigma-Aldrich, Munich, Germany) on ice for 1 h, and then 50 mM $MgCl_2 \cdot 6H_2O$ (Nacalai Tesque) was added. All recombinant proteins used in this study are shown in Figure 1.

Table 2. Primers used for cloning in this study.

name	sequence
hKPNA7 Fwd	TTTGGATCCATGCCGACCTTAGATGCTCCA
hKPNA7 Rev	CGCCTCGAGCTATTTTTTTGCTAAGCATTCATAATCTAT
mKPNA2 Fwd	AATTCCCATGTCCACGAACGAGAATG
mKPNA2 Rev	TCGAGTTAGAAGTTAAAGGTCCCAGGAG
hKPNA7 D186K Fwd	AAGGGCCCAGAGTTCAGAGATAACG
hKPNA7 from185 Rev	ACCGGCTATATTACCAAGAGCCCAC
hKPNA7 E386R Fwd	CGAGCTGTCTGGATGGTGGCGAACT
hKPNA7 from385 Rev	TTTCTGGACTTTAAATTCTCCGTTT
Flag oligonucleotide	ACCATGGACTACAAAGACCATGACGGTGATTATAAAGATCATGACATCGATTACAAGGATGACGATGACAAG
MSN Fwd	CACCATGCCCAAAACGATCAGTGTGCGTG
MSN Rev	TTACATAGACTCAAATTCGTCAATG
SORT1 Fwd	CACCATGGAGCGGCCCTGGGGAGCTGCGG
SORT1 Rev	CTATTCCAAGAGGTCCTCATCTGAG
CYFIP2Fwd	CACCATGACCACGCACGTCACCCT
CYFIP2Rev	TTAGCAAGTGGTGGCCAAGGACT
RAB3GAP2 Fwd	CACCATGGCCTGCTCCATTGTCCAGTTCT
RAB3GAP2 Rev	TCATAAAGAAGGAAGAGATATGGCT
RPTORFwd	CACCATGGAGTCCGAAATGCTGCAATC
RPTORRev	CTATCTGACACGCTTCTCCACCGAG
AIFM1 Fwd	CACCATGTTCCGGTGTGGAGGCCTGGCGG
AIFM1 Rev	TCAGTCTTCATGAATGTTGAATAGT
CCNB1 Fwd	CACCATGGCGCTCCGAGTCACCAGGAACT
CCNB1long Rev	TTACACCTTTGCCACAGCCTTGGCT
DDB2 Fwd	CACCATGGCTCCCAAGAAACGCCCAGAAA
DDB2 Rev	TCACTTCCGTGTCCTGGCTTCCTCC
FANCI Fwd	CACCATGGACCAGAAGATTTTATCTCTAG
FANCI Rev	TTATTTTTTCCTTTTCTTCTTGGCT
KDM1A Fwd	CACCATGTTATCTGGGAAGAAGGCGGCAG
KDM1A Rev	TCACATGCTTGGGGACTGCTGTGCA
KPNA3Fwd	CACCATGGCCGAGAACCCCAGCTT
KPNA3Rev	TTAAAAATTAAATTCTTTTGTTTGAAGGTTGGCTGTTGG
PELO Fwd	CACCATGAAGCTCGTGAGGAAGAACATCG
PELO Rev	TTAATCCTCTTCAGAACTGGAATCA
TELO2 Fwd	CACCATGGAGCCAGCACCCTCAGAGGTTC
TELO2 Rev	CTAGGGAGACGCGGGTGGGAGGAGC
HA oligo	ACCATGGCCTACCCATACGATGTTCCAGATTACGCTTACCCATACGATGTTCCAGATTACGCTTACCCATACGATGTTCCAGATTACGC
CCC BamHI DDB2 Fwd	CCCGGATCCATGGCTCCCAAGAAACGCCCAG
GGG BamHI C DDB2 Rev	GGGCTCGAGCTTCCGTGTCCTGGCTTCCTCCTG

Cell culture

HeLa cells and HEK293F cells were cultured in Dulbecco's modified Eagle's medium (DMEM、Sigma-Aldrich) containing 10% fetal bovine serum (FBS; GIBCO, Darmstadt, Germany) at 37 °C under an atmosphere with 10% CO_2.

Establishment of hKPNA7 and hKPNA2 stable cell lines

Stable HEK293 cell lines for constitutive expression of 3xFLAG-tagged hKPNA2 and hKPNA7 were generated using the Flp-In T-REx 293 System (Invitrogen). Cell extracts were prepared in lysis buffer (10 mM PIPES (pH 7.0), 300 mM sucrose, 1 mM $MgCl_2$, 1 mM EGTA, 0.1% Triton X-100, 0.1 mM PMSF, 1 μg/mL leupeptin) and were cleared by centrifugation. FLAG-tagged proteins were isolated by binding to anti-FLAG M2 affinity gels (Sigma-Aldrich) at 4 °C for 2 h. After washing of the gels with lysis buffer, the bound proteins were eluted and separated by sodium dodecyl sulfate-polyacrylamide gel electrophoresis (SDS-PAGE). Gel slices of each lane were excised and analyzed by mass spectrometry (MS).

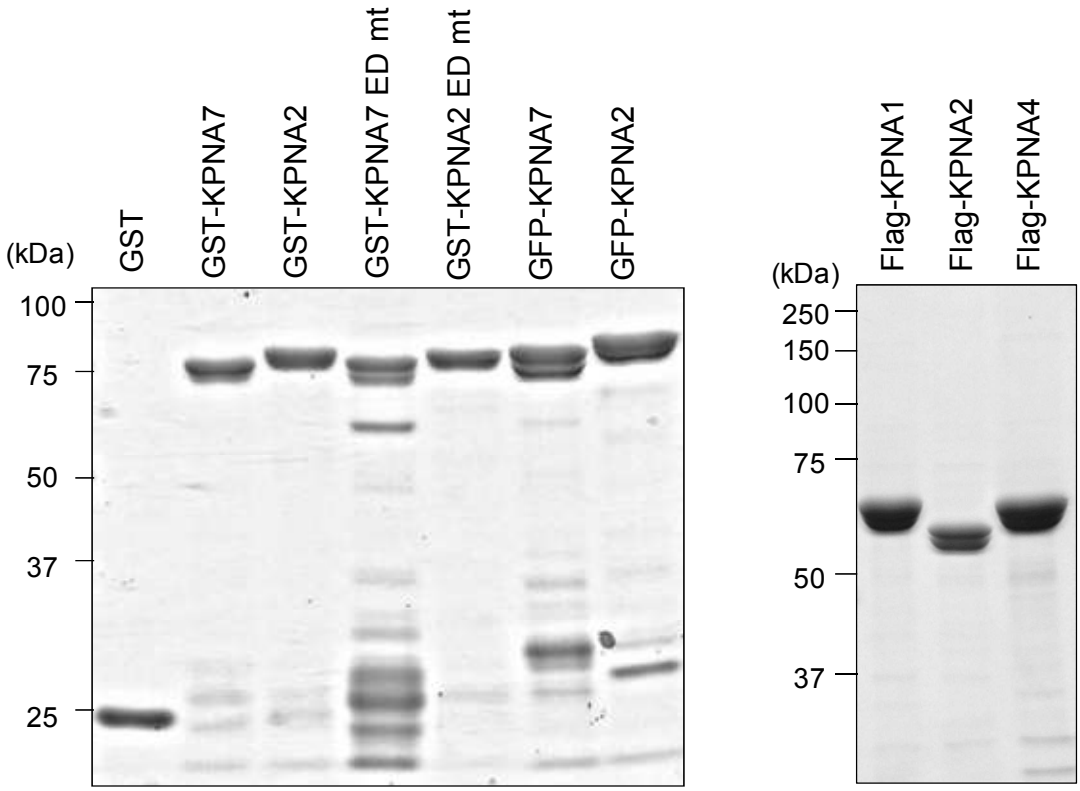

Figure 1. Recombinant proteins used in this study.

Bacterially produced recombinant proteins were separated by SDS-PAGE and stained with Coomassie blue. Per lane, 20 pmol of protein was loaded.

Mass spectrometry

Liquid chromatography/tandem mass spectrometry (LC-MS/MS) analysis was performed as described previously (Nozawa et al, 2010).

Antibodies

The following antibodies were used for western blotting: rat monoclonal anti-HA (0.1 μg/ml, Roche, Mannheim, Germany), rabbit polyclonal anti-GFP (2 μg/ml, Invitrogen), mouse monoclonal anti GST (0.2 μg/ml, Santa Cruz Biotechnology, Texas, USA), mouse monoclonal anti-karyopherin β1 (250 ng/ml, Becton, Dickinson and Company, New Jersey, USA), goat polyclonal anti-rat HRP (0.8 μg/ml, Jackson ImmunoResearch Laboratories, Pennsylvania, USA), and goat polyclonal anti-rabbit HRP (0.8 μg/ml, Jackson ImmunoResearch Laboratories). Immunofluorescence: rat monoclonal anti-HA (0.3 μg/ml, Roche), monoclonal anti-FLAG M2 antibody (15 μg/ml, Sigma) and Alexa Fluor 488-labeled donkey anti-rat IgG (2 μg/ml, Life Technologies), Alexa Fluor 594-labeled donkey anti-mouse IgG (2 μg/ml, Life Technologies), Alexa Fluor 488-labeled donkey anti-mouse IgG (2 μg/ml, Life Technologies) and Alexa Fluor 594-labeled donkey anti-rat IgG (2 μg/ml, Life Technologies).

Transfection

HEK293F cells (2.7×10^6) were plated in 100-mm dishes and HeLa cells (5×10^4) were plated in 12-well plates with cover glasses and cultured for 24 h prior to transfection. Transfection was performed with Lipofectamine 2000 Reagent (Invitrogen).

Western blotting

Western blotting was performed with cell lysates separated on an 8% SDS-PAGE gel. After the proteins were transferred onto an Immobilon-P membrane (Merck Millipore, Darmstadt, Germany) using a semidry-type blotting apparatus (ATTO, Tokyo, Japan), the membrane was blocked with blocking buffer consisting of 5% skim milk in tris-buffered saline (TBS; 20 mM Tris-HCl (pH 7.5), 150 mM NaCl) for 1 h. The membrane was probed with primary antibody diluted in blocking buffer at 4 °C overnight, and then with horseradish peroxide (HRP)-conjugated anti-rat or anti-mouse IgG at room temperature for 30 min. After washing the membrane with TBS containing 0.05% Tween-20, the protein bands were visualized with Pierce ECL Western Blotting Substrate (Thermo Scientific, Dreiech, Germany). Magic Mark XP (Invitrogen) was used as a molecular weight marker.

Binding assay using transfected HEK293F cell lysates

HEK293F cells were transfected with 3xHA-tagged bait proteins and incubated for 48 h. After

washing the cells with phosphate-buffered saline (PBS), the cells were collected in transport buffer (TB; 20 mM HEPES at pH 7.3, 110 mM potassium acetate (Nacalai Tesque), 2 mM magnesium acetate (Nacalai Tesque), 1 mM EGTA (Nacalai Tesque), 1 mM DTT, 500 μM phenylmethylsulfonyl fluoride (PMSF; Nacalai Tesque), 1 μg/ml aprotinin (Nacalai Tesque), 1 μg/ml pepstatin (Peptide Institute, Osaka, Japan), and 1 μg/ml leupeptin (Peptide Institute) with 0.1% Tween-20 (Nacalai Tesque), at 4 °C, followed by sonication for 10 s using a Sonifier 250 (output control 1, duty cycle constant; Branson, Danbury, CT, USA). The cell lysates were centrifuged at 15,000 × *g* at 4 °C for 30 min and incubated with GST-hKPNA7, GST-mKPNA2, or GST-mKPNA2ED immobilized on glutathion sepharose (GSH) beads (GE Healthcare) at 4 °C for 1 h. After incubation, the beads were washed 5 times with TB containing 0.1% Tween-20. Then, the beads were suspended in SDS-PAGE loading buffer (0.5 M Tris-HCl (pH 6.8), 34.7 mM SDS, 50 % glycerol, 25 % β-mercaptoethanol, and bromophenol). Bound proteins were analyzed by western blotting with monoclonal anti-HA antibody.

Binding assay using recombinant proteins

GFP-DDB2 and importin β1 proteins (50 pmol each) were incubated with GST, GST-hKPNA7, GST-mKPNA2, GST-hKPNA7ED, or GST-mKPNA2ED (50 pmol each) immobilized on GSH beads (GE Healthcare) in 500 μl of TB containing 0.1% Triton X-100 at 4 °C for 1 h. After the

beads were washed 5 times with TB containing 0.1% Triton X-100, they were suspended in SDS-PAGE loading buffer. Bound proteins were analyzed by western blotting with monoclonal anti-GFP or anti-importin β1 antibody.

***In vitro* nuclear transport assay**

An *in vitro* transport assay was performed as previously described (Miyamoto et al, 1997). In brief, HeLa cells were treated with 40 μg/ml digitonin (Nacalai Tesque) on ice for 5 min. Permeabilized cells were incubated in TB on ice for 5 min and washed twice with TB to minimize residual proteins in the cytoplasm. The cells were incubated at 30 °C for 30 min in TB containing 4 pmol of transport substrates such as GST-SV40T-NLS-GFP, 6 pmol of either KPNA2 or KPNA7, 4 pmol of importin β1, 40 pmol of RanGDP, and an ATP regeneration system (0.5 mM ATP (Wako), 20 U/ml creatine phosphokinase (Sigma-Aldrich), and 5 mM creatine phosphate (Sigma-Aldrich) in a total volume of 10 μl per sample. After incubation, the cells were fixed with 3.7% formaldehyde in PBS. The cells were observed under a Zeiss Axiophot 2 fluorescence microscope with a Plan-Neofluar objective lens (40×/0.75, Carl Zeiss, Oberkochen, Germany).

Immunofluorescence analysis

After 48 h of transfection, HeLa cells were fixed with 3.7% formaldehyde (Nacalai Tesque) in PBS at room temperature for 15 min and permeabilized with 0.1% Triton X-100 (Nacalai Tesque) in PBS at room temperature for 5 min. The cells were blocked with 3% skim milk in TBS with 0.05 % Tween-20 (TTBS) at room temperature for 30 min and then incubated with rat monoclonal anti-HA (Roche) and anti-FLAG M2 antibodies (Sigma) at room temperature for 90 min. After washing twice with TTBS, the cells were incubated with Alexa Fluor 488-labeled donkey anti-rat IgG and Alexa Fluor 594-labeled donkey anti-mouse IgG, or with Alexa Fluor 488-labeled donkey anti-mouse IgG and Alexa Fluor 594-labeled donkey anti-rat IgG (Life Technologies) in 3% skim milk at room temperature for 30 min. The samples were washed three times with TTBS and mounted with Duolink II mounting medium containing DAPI (Olink Bioscience, Sweden). The cells were observed under a Zeiss Axiophot 2 fluorescence microscope with a Plan-Neofluar objective lens (40×/0.75, Carl Zeiss).

RESULTS

KPNA7 can transport cNLS substrates into the nucleus

It has recently been shown that KPNA7 binds to importin β1 more efficiently than other KPNA proteins by using *in vitro* translated full-length KPNAs (Kelley et al, 2010). Based on the amino acid similarity, KPNA7 has been categorized to the KPNA2 subfamily; therefore, I characterized the function of KPNA7 by comparison with KPNA2. First, I conducted a binding assay using bacterially expressed, purified recombinant proteins. Importin β1 protein was incubated with either GST-KPNA7 or GST-KPNA2 immobilized on the GSH beads and the bound protein was detected by western blotting using anti-importin β1 antibody. Figure 2A shows that KPNA7 bound to importin β1 more efficiently than KPNA2.

In addition, it has been reported that KPNA7 is able to bind to the retinoblastoma NLS, but not to the SV40T-NLS (Kelley et al, 2010). Amino acid sequence alignment analysis of KPNA7 and KPNA2 revealed that the critical amino acids in the major and minor NLS-binding sites (Fontes et al, 2000) are conserved between these two proteins (Figure 3), suggesting that KPNA7 has a potential for interacting with cNLSs such as SV40T-NLS. Therefore, I examined whether KPNA7 binds to SV40T-NLS using a GST pull-down assay. Bacterially produced GST-KPNA7 and GST-KPNA2 were purified and immobilized on the GSH beads, and incubated with the SV40T-NLS-GFP fusion protein. Proteins bound to the GST-KPNAs

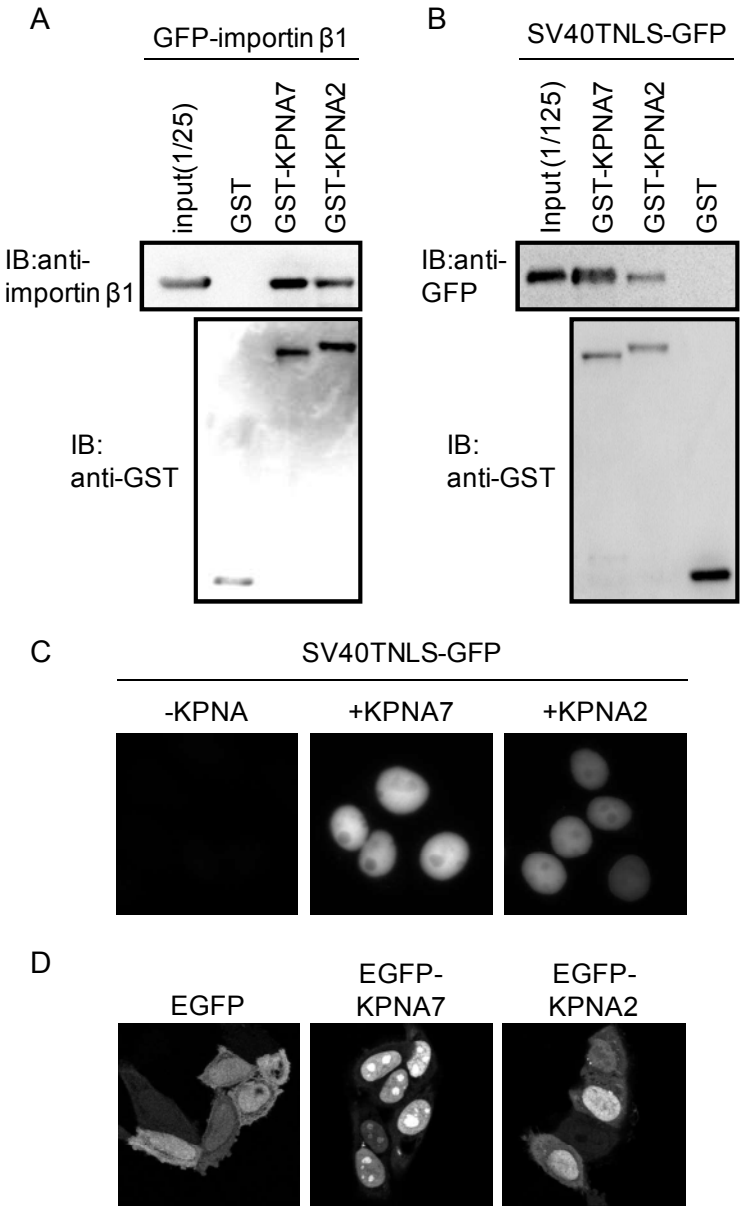

Figure 2. KPNA7 has an ability to transport SV40T-NLS-substrates into the nucleus in an importin β1- and Ran-dependent manner.

A. GST, GST-KPNA7, and GST-KPNA2 (50 pmol each) were immobilized on GSH beads and incubated with recombinant importin β1 (50 pmol). Bound proteins were detected with anti-importin β1 and anti-GST. B. GST, GST-KPNA7, and GST-KPNA2 (50 pmol each) were immobilized on GSH beads and incubated with SV40T-NLS-GFP recombinant protein (50 pmol). Bound proteins were detected with anti-GFP and anti-GST. C. An *in vitro* transport assay was performed to examine the nuclear transport activity of KPNA7. Digitonin-permeabilized HeLa cells were incubated with GST-SV40T-NLS-GFP, importin β1, RanGDP,

NTF2, and an ATP regenerative system with or without KPNA7 or KPNA2. After incubation for 15 min, the cells were observed using a fluorescence microscope. D. HeLa cells were transfected with plasmids encoding EGFP, EGFP-KPNA7, or EGFP-KPNA2. After a 24-h culture, GFP fluorescence was observed using a fluorescence microscope.

A

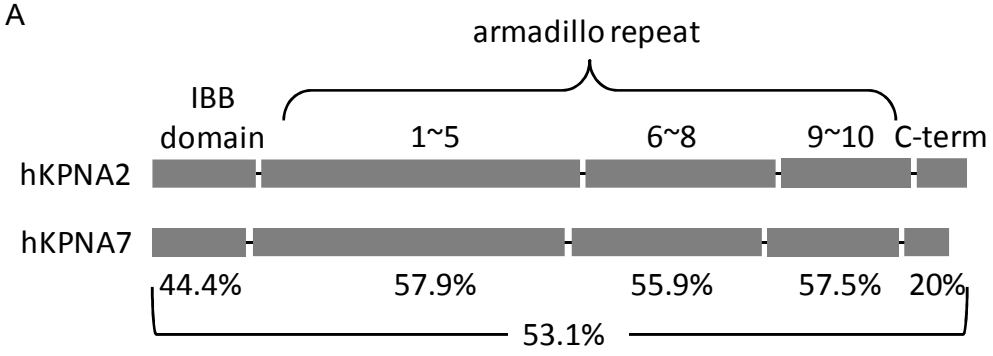

B

```
KPNA2           MSTNENANTPAARLHRFKNKGKDSTEMRRRRIEVNVELRKAKKDDQMLKRRNVSSFPDDA
KPNA7           ---MPTLDAPEERRRKFKYRGKDVSLRRQQRMAVSLELRKAKKDEQTLKRRNITSFCPDT
                     . ::*  * ::** :*** :  *::*: *.:********:* *****::**  *:
KPNA2           TSPLQENRNNQGTVNWSVDDIVKGINSSNVENQLQATQAARKLLSREKQPPIDNIIRAGL
KPNA7           PS---EKTAKGVAVSLTLGEIIKGVNSSDPVLCFQATQTARKMLSQEKNPPLKLVIEAGL
                .*   *:  :  :*. ::.:*:**:***:    :****:***:**:**:**:. :*.***
KPNA2           IPKFVSFLGRTDCSPIQFESAWALTNIASGTSEQTKAVVDGGAIPAFISLLASPHAHISE
KPNA7           IPRMVEFLKSSLYPCLQFEAAWALTNIASGTSEQTRAVVEGGAIQPLIELLSSSNVAVQE
                **.:*.**  :  . :***:***************:***:**** .:*.**:*.:  :.*
KPNA2           QAVWALGNIAGDGSVFRDLVIKYGAVDPLLALLAVPDMSSLACGYLRNLTWTLSNLCRNK
KPNA7           QAVWALGNIAGDGPEFRDNVITSNAIPHLLALISP----TLPITFLRNITWTLSNLCRNK
                *************. *** **. .*:  ****::     :*.  :***:***********
KPNA2           NPAPPIDAVEQILPTLVRLLHHDDPEVLADTCWAISYLTDGPNERIGMVVKTGVVPQLVK
KPNA7           NPYPCDTAVKQILPALLHLLQHQDSEVLLDACWALSYLTDGSNKRIGQVVNTGVLPRLVV
                ** *   **:****:*::**:*:* ***:*:***:******.*:*** **:***:*:**
KPNA2           LLGASELPIVTPAIRAIGNIVTGTDEQTQVVIDAGALAVFPSLLTNPKTNIQKEATWTMS
KPNA7           LMTSSELNVLTPSLRTVGNIVTGTDEQTQMAIDAGMLNVLPQLLQHNKPSIQKEAAWALS
                *: :*** ::**:**::************:.**** * *:*.** : *..******::*:*
KPNA2           NITAGRQDQIQQVVNHGLVPFLVSVLSKADFKTQKEAVWAVTNYTSGGTVEQIVYLVHCG
KPNA7           NVAAGPCHHIQQLLAYDVLPPLVALLKNGEFKVQKEAVWMVANFATGATMDQLIQLVHSG
                *::**  .:***:: :.::* **::*.:.:**.****** *:*:::*.*::*:: ***.*
KPNA2           IIEPLMNLLTAKDTKIILVILDAISNIFQAAEKLGETEKLSIMIEECGGLDKIEALQNHE
KPNA7           VLEPLVNLLTAPDVKIVLIILDVISCILQAAEKRSEKENLCLLIEELGGIDRIEALQLHE
                ::***:***** *.**:*:***.** *:***** .*.*:*.::*** **:*:***** **
KPNA2           NESVYKASLSLIEKYFSVEEEEDQNVVPETTSEGYTFQVQDGAPGTFNF
KPNA7           NRQIGQSALNIIEKHFGEEEDESQTLLSQVIDQDYEFIDYECLAKK---
                *..: :::*.:***:*. **:*.*.::.:. .::* *   :  . .
```

Figure 3. Homology between human KPNA7 and human KPNA2.

A. The amino acid similarity between hKPNA7 and hKPNA2 was assessed using CLUSTALW (http://www.genome.jp/tools/clustalw/). The IBB domain: 1~63 of KPNA7 and 1~69 of KPNA2, ARM repeats 1~5: 64~272 of KPNA7 and 70~282 of KPNA2, ARM repeats 6~8: 273~399 of KPNA7 and 283~409 of KPNA2, ARM repeats 9~10: 400~486 of KPNA7 and 410~496 of KPNA2, C-term: 487~516 of KPNA7 and 497~529 of KPNA2. B. Sequence alignment of hKPNA7 and hKPNA2. Critical amino acids in the NLS binding pockets of hKPNA2 are conserved in hKPNA7 and are indicated in the black frame.

produced GST-KPNA7 and GST-KPNA2 were purified and immobilized on the GSH beads, and incubated with the SV40T-NLS-GFP fusion protein. Proteins bound to the GST-KPNAs were subsequently detected by western blotting using anti-GFP antibody. The results demonstrated that GST-KPNA7 bound to SV40T-NLS-GFP more efficiently than KPNA2 (Figure 2B). In addition, the NLS interaction defective mutants of KPNAs (ED mutants: D192K/E396R in KPNA2 and D186K/E386R in KPNA7) showed only weak binding to the SV40T-NLS substrate (data not shown). These results strongly suggest that, like KPNA2, KPNA7 functions as a cNLS receptor.

To confirm this hypothesis, I examined the nuclear transport activity of KPNA7 using an *in vitro* transport assay. After HeLa cells were permeabilized with digitonin, the nuclear migration of the cNLS substrate was examined in the presence of either KPNA7 or KPNA2 together with importin β1, RanGDP, NTF2, and an ATP regeneration system. The results showed that GST-SV40T-NLS-GFP was efficiently transported into the nucleus of HeLa cells in the KPNA7- as well as the KPNA2-dependent manner (Figure 2C).

Identification of KPNA7- and KPNA2-binding proteins

Although KPNA7 has been classified to the KPNA2 subfamily, the amino acid similarity between hKPNA7 and hKPNA2 is quite low (55%) compared to that between other subfamily

members (e.g., 85% between KPNA3 and KPNA4), suggesting functional divergence of these two proteins. To assess this, I attempted to identify KPNA7- and KPNA2-binding proteins in Flp-In 293 cell lines stably expressing FLAG-KPNA7 or FLAG-KPNA2 using FLAG-immunoprecipitation followed by LC-MS/MS analysis (Table 3). A total of 179 and 133 proteins were found to bind to KPNA7 and KPNA2, respectively, of which only 62 proteins bound to both KPNA2 and KPNA7 (Figure 4A).

Web-based analysis of the KPNA-binding proteins

To search for cNLSs in the candidate KPNA-binding proteins, the cNLS Mapper software (http://nls-mapper.iab.keio.ac.jp/cgi-bin/NLS_Mapper_form.cgi) (Kosugi et al, 2009) was used. The highest score for each candidate is indicated in Table 3. Based on the scores, the proteins were categorized as "High" (≥ 6) or "Low" (< 6) (Figure 4B). There were no major differences between KPNA7 and KPNA2 in the scores of the binding partners.

Next, I assessed the subcellular localization of the candidates by PSORT II (Nakai & Horton, 1999). The localizations with the highest prediction scores for each candidate are presented in the Figure 4C. The majority of the candidates are predicted to localize in the cytoplasm or the nucleus. Eight percent and 6% of the KPNA7-binding and 11% and 5% of KPNA2-binding partners were predicted to localize in the mitochondria and the endoplasmic

Table 3. List of KPNA2- and KPNA7-binding proteins.

Name	Symbol	Acc. No.	M.W. (KDa)	KPNA7	KPNA2	Higest score
Importin subunit alpha-8	KPNA7	IPI00374362	57	220	18	5.8
Importin subunit beta-1	KPNB1	IPI00001639	97	70	76	3.2
Importin-7	IPO7	IPI00007402	120	60	11	4.0
Nuclear cap-binding protein subunit 1	NCBP1	IPI00019380	92	14	39	15.4
Proteasome activator complex subunit 3	PSME3	IPI00030243	30	3	42	12.5
Nuclear pore complex protein Nup153	NUP153	IPI00292059	154	0	40	4.6
Nucleoporin 50 kDa	NUP50	IPI00026940	50	0	32	4.0
mRNA cap guanine-N7 methyltransferase	RNMT	IPI00410657	58	2	26	12.0
cDNA FLJ78440, highly similar to Human lactoferrin	LTF	IPI00298860	78	0	15	4.4
Signal recognition particle 54 kDa protein	SRP54	IPI00009822	56	9	6	4.8
mRNA-capping enzyme	RNGTT	IPI00000104	69	9	6	16.9
Beta-catenin-like protein 1	CTNNBL1	IPI00844214	65	10	4	7.5
Chromodomain-helicase-DNA-binding protein 8	CHD8	IPI00398992	291	10	2	10.0
Nucleolar protein 58	NOP58	IPI00006379	60	2	11	11.5
Cation-independent mannose-6-phosphate receptor	IGF2R	IPI00289819	274	9	1	6.5
Phosphorylated adapter RNA export protein	PHAX	IPI00303402	44	6	7	7.0
Histone-binding protein RBBP4	RBBP4	IPI00328319	48	2	8	3.8
WD repeat and HMG-box DNA-binding protein 1	WDHD1	IPI00411614	126	0	11	7.0
Protein SET	SET	IPI00072377	33	5	3	7.0
Afadin	MLLT4	IPI00023461	207	8	0	8.0
Exportin-2	CSE1L	IPI00022744	110	6	2	6.5
Isoform GTBP-N of DNA mismatch repair protein Msh6	MSH6	IPI00384456	153	3	3	11.0
Mannosyl-oligosaccharide glucosidase	MOGS	IPI00328170	92	8	2	3.2
Trifunctional enzyme subunit alpha, mitochondrial	HADHA	IPI00031522	83	5	2	5.0
La-related protein 7	LARP7	IPI00294742	68	2	5	13.8
SWI/SNF-related matrix-associated actin-dependent regulator of chromatin a4 isoform D	SMARCA4	IPI00029822	188	0	9	14.0
Sortilin	SORT1	IPI00217882	92	9	0	5.4
Tripartite motif-containing protein 25	TRIM25	IPI00029629	71	7	2	5.6
V-type proton ATPase catalytic subunit A	ATP6V1A	IPI00007682	68	3	5	3.7
Kinetochore-associated protein 1	KNTC1	IPI00001458	251	6	1	7.0
SWI/SNF complex subunit SMARCC2	SMARCC2	IPI00150057	125	0	6	11.0
Vimentin	VIM	IPI00418471	54	0	8	3.6
Rab3 GTPase-activating protein non-catalytic subunit	RAB3GAP2	IPI00554590	156	8	0	4.6
tRNA (cytosine-5-)-methyltransferase NSUN2	NSUN2	IPI00306369	86	8	0	12.0
STE20-like serine/threonine-protein kinase	SLK	IPI00022827	143	3	2	8.2
Eukaryotic peptide chain release factor subunit 1	ETF1	IPI00429191	49	1	4	3.8
Ras GTPase-activating-like protein IQGAP3	IQGAP3	IPI00328905	185	5	0	6.7
6-phosphofructokinase, liver type	PFKL	IPI00332371	85	2	5	4.0
NMDA receptor-regulated protein 1	NAA15	IPI00386189	101	6	2	7.9
Isoform Long of Delta-1-pyrroline-5-carboxylate synthetase	ALDH18A1	IPI00008982	87	2	3	3.7
Ankyrin-2	ANK2	IPI00007834	430	7	0	10.0
Uncharacterized protein KIAA1797	FOCAD	IPI00748360	200	3	1	4.1
Disco-interacting protein 2 homolog B	DIP2B	IPI00465045	171	3	2	6.9
Actin-related protein 2	ACTR2	IPI00005159	45	2	3	3.9
Threonyl-tRNA synthetase, cytoplasmic	TARS	IPI00329633	83	3	0	4.1
DNA-directed RNA polymerase III subunit RPC3	POLR3C	IPI00007948	61	3	3	18.0
General transcription factor IIF subunit 1	GTF2F1	IPI00017450	58	4	4	10.5
Prohibitin	PHB	IPI00017334	30	0	6	3.3
Putative uncharacterized protein DKFZp686J11235 (Fragment)	IGHA1	IPI00426060	54	0	6	3.6
Gamma-glutamyl hydrolase	GGH	IPI00023728	36	2	2	3.9
Importin subunit alpha-3	KPNA3	IPI00299033	58	6	0	5.6
Extended synaptotagmin-1	ESYT1	IPI00022143	123	6	0	7.1
WD repeat-containing protein 26	WDR26	IPI00414197	72	3	3	6.0
AP-2 complex subunit beta-1	AP2B1	IPI00784156	105	3	3	5.2
Histidyl-tRNA synthetase, cytoplasmic	HARS	IPI00021808	57	2	3	5.4
Putative pre-mRNA-splicing factor ATP-dependent RNA helicase DHX15	DHX15	IPI00396435	91	3	2	11.5
Serine/threonine-protein kinase 38-like	STK38L	IPI00237011	54	0	3	5.8

Microtubule-actin cross-linking factor 1, isoforms 1/2/3/5	MACF1	IPI00256861	620	4	0	9.0
Melanoma-associated antigen D2	MAGED2	IPI00009542	65	6	0	4.2
cDNA FLJ44241 fis, clone THYMU3008436, highly similar to 6-phosphofructokinase, muscle type	PFKM	IPI00465179	93	2	0	5.8
Prenylcysteine oxidase-like	PCYOX1L	IPI00184180	55	6	0	4.7
Dihydropyrimidinase-like 2	SDF2L1	IPI00106642	67	3	0	3.2
Acidic leucine-rich nuclear phosphoprotein 32 family member A	ANP32A	IPI00025849	29	1	2	11.0
Ribonuclease P protein subunit p30	RPP30	IPI00019196	29	1	1	8.1
Creatine kinase, ubiquitous mitochondrial	CKMT1A	IPI00658109	47	3	0	4.9
Glutamate-rich WD repeat-containing protein 1	GRWD1	IPI00027831	49	2	3	4.3
Huntingtin	HTT	IPI00002335	348	1	2	7.1
Ewing sarcoma breakpoint region 1 isoform 1	EWSR1	IPI00009841	69	3	0	3.9
HBS1-like protein	HBS1L	IPI00009070	75	1	3	6.8
DNA polymerase	POLE	IPI00744598	263	3	0	12.0
Superkiller viralicidic activity 2-like 2	SKIV2L2	IPI00647217	118	2	0	8.0
Moesin	MSN	IPI00219365	68	3	0	5.4
Dynamin-like 120 kDa protein, mitochondrial	OPA1	IPI00006721	112	3	1	7.4
Dolichyl-diphosphooligosaccharide--protein glycosyltransferase 48 kDa subunit	DDOST	IPI00297084	51	0	2	3.8
1-phosphatidylinositol-4,5-bisphosphate phosphodiesterase gamma-1	PLCG1	IPI00016736	149	2	1	4.5
Protein SGT1	ECD	IPI00027034	73	4	3	4.8
Methionyl-tRNA synthetase, cytoplasmic	MARS	IPI00008240	101	3	2	6.3
Heterogeneous nuclear ribonucleoprotein U-like protein 2	HNRNPUL2	IPI00456887	85	4	1	5.4
Estradiol 17-beta-dehydrogenase 12	HSD17B12	IPI00007676	34	4	0	Non
DNA-directed RNA polymerase III subunit RPC1	POLR3A	IPI00024163	156	0	5	5.1
Full-length cDNA clone CS0DI031YK16 of Placenta of Homo sapiens	TDP1	IPI00384157	42	0	5	Non
cDNA FLJ56425, highly similar to Very-long-chain specific acyl-CoAdehydrogenase, mitochondrial	ACADVL	IPI00028031	75	5	0	4.8
Serine/arginine repetitive matrix protein 2	SRRM2	IPI00782992	300	0	3	14.0
Fermitin family homolog 2	FERMT2	IPI00000856	78	1	4	5.5
cDNA FLJ75085, highly similar to Homo sapiens glutaminyl-tRNA synthetase (QARS), mRNA	QARS	IPI00026665	90	0	1	5.0
Eukaryotic translation initiation factor 1	EIF1	IPI00015077	13	1	1	6.0
Malignant T cell amplified sequence 1	MCTS1	IPI00900380	19	0	1	3.8
Fructose-bisphosphate aldolase	ALDOC	IPI00418262	48	0	3	3.1
Nucleolar protein 56	NOP56	IPI00411937	66	2	2	10.5
Putative heat shock protein HSP 90-beta 4	HSP90AB4P	IPI00555565	58	3	0	4.9
SF3A2 protein (Fragment)	SF3A2	IPI00017341	51	1	1	8.0
Protein LYRIC	MTDH	IPI00328715	64	4	0	7.0
3-ketoacyl-CoA thiolase, peroxisomal	ACAA1	IPI00012828	44	1	1	4.7
cDNA FLJ53229, highly similar to Importin alpha-7 subunit	KPNA6	IPI00747764	61	0	3	4.7
ADP-ribosylation factor-like protein 6-interacting protein 4	ARL6IP4	IPI00434965	38	0	4	11.5
Annexin VI isoform 2	ANXA6	IPI00002459	75	0	3	6.4
Notchless protein homolog 1	NLE1	IPI00018196	53	3	2	3.6
Mitochondrial import inner membrane translocase subunit TIM50	TIMM50	IPI00418497	50	4	2	6.0
Isocitrate dehydrogenase 3, beta subunit isoform a precursor	IDH3B	IPI00304417	43	3	2	Non
Prostaglandin E synthase 2	PTGES2	IPI00303568	42	2	2	4.5
Isoform alpha-enolase of Alpha-enolase	ENO1	IPI00465248	47	0	3	3.5
Radixin, isoform CRA_a	RDX	IPI00017367	71	3	1	5.6
H/ACA ribonucleoprotein complex subunit 4	DKC1	IPI00221394	58	0	3	10.0
Cytoplasmic FMR1-interacting protein 2	CYFIP2	IPI00719600	146	2	0	6.5
Nicotinamide phosphoribosyltransferase	NAMPT	IPI00018873	56	0	3	5.1
Isoform Long of Cold shock domain-containing protein E1	CSDE1	IPI00470891	89	0	3	6.1
Exportin-1	XPO1	IPI00298961	123	6	0	4.1
12 kDa protein	RPL36	IPI00940035	12	4	0	10.0
Carbonyl reductase [NADPH] 1	CBR1	IPI00295386	30	0	5	3.5
Structural maintenance of chromosomes protein 1A	SMC1A	IPI00291939	143	3	0	10.5
Probable methyltransferase TARBP1	TARBP1	IPI00298447	182	3	0	7.0
Aminoacyl tRNA synthetase complex-interacting multifunctional protein 2	AIMP2	IPI00011916	35	1	0	3.1
Protein HEXIM1	HEXIM1	IPI00007941	41	0	3	10.0
tRNA (adenine-N(1)-)-methyltransferase catalytic subunit TRMT61A	TRMT61A	IPI00783197	31	2	1	Non
Hydroxysteroid dehydrogenase-like protein 2	HSDL2	IPI00414384	45	2	2	4.5
Pseudouridylate synthase 7 homolog	PUS7	IPI00044761	75	3	0	7.0
Nodal modulator 1	NOMO1	IPI00329352	134	1	1	4.6

Ribosomal RNA processing protein 1 homolog A	RRP1	IPI00550766	53	2	0	6.3
Proteasome subunit beta type-6	PSMB6	IPI00000811	25	1	0	Non
Lamina-associated polypeptide 2, isoform alpha	TMPO	IPI00216230	75	0	3	9.0
ATP-binding cassette sub-family F member 2	ABCF2	IPI00005045	71	2	0	5.5
Family with sequence similarity 98, member B isoform 1	FAM98B	IPI00760837	46	2	0	Non
RNA-binding protein 4	RBM4	IPI00003704	40	3	0	3.2
Myotubularin-related protein 5	SBF1	IPI00218397	212	2	0	4.4
Zinc phosphodiesterase ELAC protein 2	ELAC2	IPI00396627	92	1	2	7.0
cDNA FLJ56414, highly similar to Homo sapiens proline-, glutamic acid-, leucine-rich protein 1 (PELP1), mRNA	PELP1	IPI00006702	125	2	0	6.0
HZGJ	WDR92	IPI00465211	85	2	0	4.2
Regulatory-associated protein of mTOR	RPTOR	IPI00166044	149	3	0	4.1
Probable ATP-dependent RNA helicase DHX36	DHX36	IPI00784170	113	0	2	7.0
Cell division protein kinase 2	CDK2	IPI00031681	34	0	2	4.5
40S ribosomal protein S29	RPS29	IPI00182289	7	0	2	Non
Keratin, type II cytoskeletal 8	KRT8	IPI00554648	54	0	3	4.0
Phosphoglycerate mutase family member 5	PGAM5	IPI00788907	32	0	2	6.9
Nucleolar GTP-binding protein 1	GTPBP4	IPI00385042	74	2	0	12.0
Kinesin-like protein KIF1C	KIF1C	IPI00179757	123	4	0	6.5
Kinesin-like protein KIFC1	KIFC1	IPI00306400	74	0	5	14.3
ATP synthase subunit O, mitochondrial	ATP5O	IPI00007611	23	0	1	4.8
Vacuolar protein sorting-associated protein 29	VPS29	IPI00170796	21	2	0	3.3
Spindlin-1	SPIN1	IPI00550655	30	0	2	4.8
Peroxisomal acyl-coenzyme A oxidase 1	ACOX1	IPI00296907	74	2	0	4.6
ANKHD1-EIF4EBP3 protein	ANKHD1	IPI00217442	277	2	0	6.6
TBC1 domain family member 4	TBC1D4	IPI00220901	147	2	0	6.5
Probable ATP-dependent RNA helicase DDX17	DDX17	IPI00889541	80	2	0	6.0
Activating signal cointegrator 1 complex subunit 2	ASCC2	IPI00549736	86	1	0	9.5
Probable E3 ubiquitin-protein ligase HERC2	HERC2	IPI00005826	527	0	1	8.5
Aspartate aminotransferase, mitochondrial	GOT2	IPI00018206	47	0	2	4.4
Protein FAM91A1	FAM91A1	IPI00152671	94	2	0	4.5
Spermatogenesis-associated protein 5	SPATA5	IPI00329583	98	2	0	4.9
Obg-like ATPase 1	OLA1	IPI00290416	45	1	0	3.4
Melanoma inhibitory activity protein 3	MIA3	IPI00455473	214	0	1	6.1
Signal recognition particle receptor subunit beta	SRPRB	IPI00295098	30	2	0	3.8
Metastasis-associated protein MTA2	MTA2	IPI00171798	75	1	0	7.4
cDNA FLJ53324, highly similar to Tight junction protein ZO-2	TJP2	IPI00003843	137	1	0	5.6
Protein transport protein Sec23B	SEC23B	IPI00017376	86	0	2	4.0
Protein pelota homolog	PELO	IPI00106698	43	2	0	9.0
Abnormal spindle-like microcephaly-associated protein	ASPM	IPI00743813	410	1	0	11.2
Quinone oxidoreductase	CRYZ	IPI00000792	35	2	0	Non
Ribonuclease P protein subunit p40	RPP40	IPI00332091	39	2	0	4.2
RNA polymerase II-associated protein 3	RPAP3	IPI00002408	76	2	0	5.9
Putative RNA-binding protein Luc7-like 1	LUC7L	IPI00071318	44	2	0	5.5
Lipocalin-1	LCN1	IPI00009650	19	0	4	3.5
Replication factor C subunit 2	RFC2	IPI00017412	39	2	0	4.5
RNA polymerase-associated protein CTR9 homolog	CTR9	IPI00477468	134	2	0	13.0
Large proline-rich protein BAT3	BAG6	IPI00465128	119	0	3	9.0
GTP-binding nuclear protein Ran	RAN	IPI00643041	24	0	1	4.6
U4/U6.U5 tri-snRNP-associated protein 2	USP39	IPI00419844	65	2	0	6.4
EF-hand domain-containing family member A1	EFHA1	IPI00640276	50	3	0	4.5
Histone deacetylase 2	HDAC2	IPI00289601	66	0	2	6.2
Apoptosis-inducing factor 1, mitochondrial	AIFM1	IPI00000690	67	4	0	3.8
DNA damage-binding protein 2	DDB2	IPI00021518	48	4	0	14.5
Phosphoglycerate kinase 1	PGK1	IPI00169383	45	0	3	3.6
Alkyldihydroxyacetonephosphate synthase, peroxisomal	AGPS	IPI00010349	73	2	0	4.7
Origin recognition complex subunit 6	ORC6	IPI00001641	28	1	0	16.5
Small nuclear ribonucleoprotein G	SNRPG	IPI00016572	8	0	1	Non
U6 snRNA-associated Sm-like protein LSm4	LSM4	IPI00294955	15	1	0	3.1
Uncharacterized protein C1orf77	CHTOP	IPI00300990	26	0	1	3.5
34 kDa protein	SLC25A11	IPI00796094	34	0	1	3.5
Serine hydroxymethyltransferase, mitochondrial	SHMT2	IPI00002520	56	0	2	3.6
Heterogeneous nuclear ribonucleoprotein F	HNRNPF	IPI00003881	46	2	0	Non
Cyclin B1	CCNB1	IPI00294696	44	2	0	5.3
SET domain-containing protein 3	SETD3	IPI00165026	67	1	0	6.5
Bifunctional methylenetetrahydrofolate dehydrogenase/cyclohydrolase, mitochondrial	MTHFD2	IPI00011307	38	0	2	5.5

Glycogen synthase kinase-3 alpha	GSK3A	IPI00292228	51	0	1	3.6
Isoform Alpha of Nuclear inhibitor of protein phosphatase 1	PPP1R8	IPI00030383	38	1	0	13.5
DNA topoisomerase 2-alpha	TOP2A	IPI00218753	179	0	1	7.2
S-adenosylmethionine synthetase isoform type-2	MAT2A	IPI00010157	44	1	0	3.5
DnaJ homolog subfamily B member 1	DNAJB1	IPI00015947	38	2	0	6.6
PCI domain-containing protein 2	PCID2	IPI00072541	43	0	1	4.3
Nuclear cap-binding protein subunit 2	NCBP2	IPI00183500	18	0	1	Non
39S ribosomal protein L46, mitochondrial	MRPL46	IPI00023161	32	0	1	4.3
cDNA FLJ55574, highly similar to Calnexin	CANX	IPI00020984	72	1	0	5.2
Tetratricopeptide repeat protein 28	TTC28	IPI00879193	271	2	0	4.4
Coiled-coil domain-containing protein 147	CCDC147	IPI00174574	103	1	0	6.1
Replication factor C subunit 3	RFC3	IPI00031521	41	0	1	4.0
Telomere length regulation protein TEL2 homolog	TELO2	IPI00016868	92	2	0	4.6
Lamin-B1	LMNB1	IPI00217975	66	1	0	8.5
Isoform CNPI of 2',3'-cyclic-nucleotide 3'-phosphodiesterase	CNP	IPI00220993	45	1	0	4.0
Phosphoinositide 3-kinase regulatory subunit 4	PIK3R4	IPI00024006	153	1	0	7.5
Replication protein A 32 kDa subunit	RPA2	IPI00013939	29	0	3	3.5
DNA mismatch repair protein Mlh1	MLH1	IPI00029754	85	0	3	8.0
Long-chain-fatty-acid--CoA ligase 3	ACSL3	IPI00031397	80	3	0	9.2
Sorting nexin-2	SNX2	IPI00299095	58	3	0	4.6
DNA-directed RNA polymerase III subunit RPC2	POLR3B	IPI00301346	128	0	3	7.3
Isovaleryl-CoA dehydrogenase, mitochondrial	IVD	IPI00645805	46	3	0	Non
Methyl-CpG-binding domain protein 3	MBD3	IPI00439194	33	0	2	5.6
Stromal antigen 2 isoform a	STAG2	IPI00470883	146	0	1	8.6
Transcription initiation factor TFIID subunit 9	TAF9	IPI00002993	29	0	2	8.0
Lysozyme C	LYZ	IPI00019038	17	0	1	Non
2-oxoglutarate and iron-dependent oxygenase domain-containing protein 1	OGFOD1	IPI00170429	63	0	2	7.1
Zinc finger ZZ-type and EF-hand domain-containing protein 1	ZZEF1	IPI00385631	331	0	2	8.5
Protein diaphanous homolog 1	DIAPH1	IPI00852685	141	2	0	6.0
Serine hydroxymethyltransferase, cytosolic	SHMT1	IPI00002519	53	0	2	4.9
Serine/threonine-protein kinase WNK1	WNK1	IPI00004472	251	2	0	7.5
Carnitine O-palmitoyltransferase 2, mitochondrial	CPT2	IPI00012912	74	2	0	4.8
WD repeat domain phosphoinositide-interacting protein 3	WDR45B	IPI00021329	38	0	2	6.4
GMP synthase [glutamine-hydrolyzing]	GMPS	IPI00029079	77	0	2	4.2
Sphingosine-1-phosphate lyase 1	SGPL1	IPI00099463	64	2	0	7.1
Aspartyl-tRNA synthetase, mitochondrial	DARS2	IPI00100460	74	2	0	3.8
FtsJ methyltransferase domain-containing protein 2	FTSJD2	IPI00166153	95	2	0	9.0
Importin-9	IPO9	IPI00185146	116	2	0	5.0
Lysine-specific histone demethylase 1	KDM1A	IPI00217540	95	2	0	11.0
Protein TMED8	TMED8	IPI00292812	46	2	0	3.5
Aspartyl/asparaginyl beta-hydroxylase	ASPH	IPI00294834	86	2	0	6.1
Isoform Alpha of Vinexin	SORBS3	IPI00419847	75	2	0	6.6
Serine/threonine-protein kinase MRCK beta	CDC42BPB	IPI00477763	194	2	0	6.0
Neurochondrin	NCDN	IPI00549543	79	2	0	5.3
HLA class I histocompatibility antigen, Cw-7 alpha chain	HLA-C	IPI00642409	41	2	0	3.3
Inverted formin-2	INF2	IPI00876962	135	2	0	6.1
Phosphatidylinositol-3,4,5-trisphosphate 5-phosphatase 2	INPPL1	IPI00016932	139	1	0	7.2
Heat shock 70 kDa protein 14	HSPA14	IPI00292499	55	0	1	3.2
Putative uncharacterized protein ALB	ALB	IPI00022434	72	0	1	6.6
Zinc finger CCCH-type antiviral protein 1	ZC3HAV1	IPI00332936	78	1	0	4.0
Trafficking protein particle complex subunit 10	TRAPPC10	IPI00298870	142	1	0	4.5
cDNA FLJ54536, highly similar to Mitochondrial 28S ribosomal protein S27	MRPS27	IPI00022002	49	0	1	4.2
LanC-like protein 2	LANCL2	IPI00032995	51	1	0	4.0
Leucine-rich repeat-containing protein 40	LRRC40	IPI00152998	68	1	0	4.5
SAM domain and HD domain-containing protein 1	SAMHD1	IPI00294739	72	1	0	10.0
Septin 9 isoform a	SEPT9	IPI00784614	65	1	0	5.2
Cullin-1	CUL1	IPI00014310	90	1	0	6.7
Probable ATP-dependent RNA helicase DDX52	DDX52	IPI00032423	67	1	0	10.0
Dolichyl-phosphate beta-glucosyltransferase	ALG5	IPI00002506	37	1	0	4.9
54 kDa protein	SMARCD2	IPI00177890	54	0	1	11.5
Polymerase delta-interacting protein 2	POLDIP2	IPI00165506	42	1	0	3.8
CTP synthase 1	CTPS1	IPI00290142	67	1	0	6.4
Serine/threonine-protein kinase RIO3	RIOK3	IPI00298199	59	1	0	4.5
Nucleolar RNA helicase 2	DDX21	IPI00015953	87	1	0	12.5
Ran-binding protein 9	RANBP9	IPI00465275	78	1	0	6.2
Chitinase domain-containing protein 1	CHID1	IPI00045536	42	1	0	5.2
Vacuolar protein sorting-associated protein 45	VPS45	IPI00090327	65	1	0	6.3
Proliferating cell nuclear antigen	PCNA	IPI00021700	29	1	0	Non

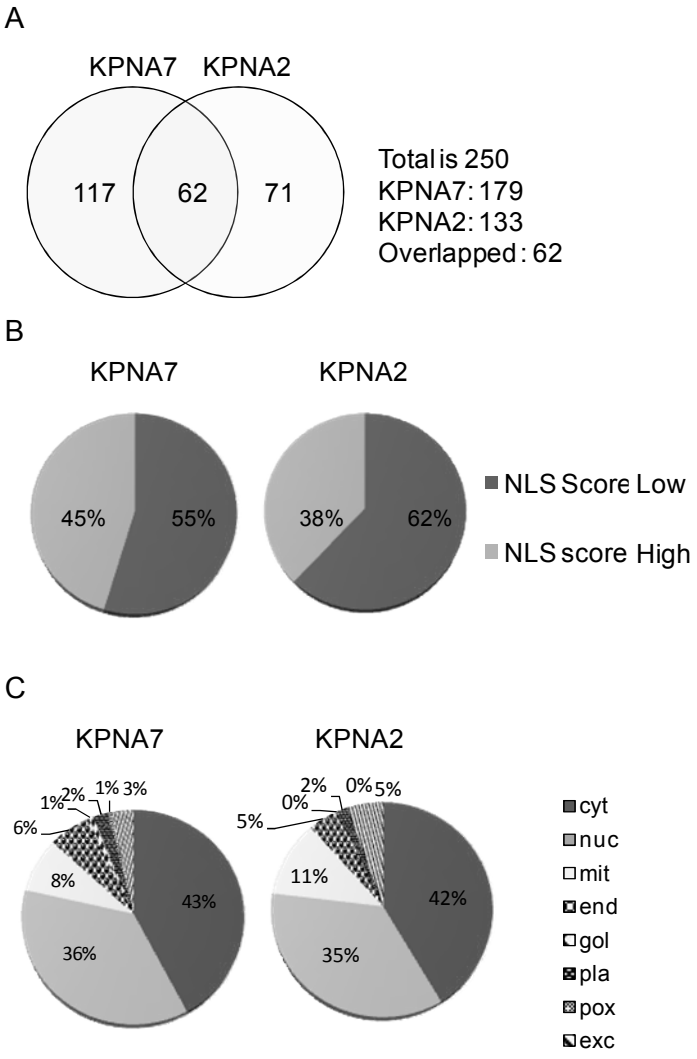

Figure 4. Identification of KPNA7- and KPNA2-binding proteins.

A. Venn diagram grouping candidate KPNA7- and KPNA2-binding proteins as identified by mass spectroscopy (MS). The proteins are classified as binding to KPNA7, KPNA2, and both KPNA7 and KPNA2. B. Pie chart of the composition of the candidates possessing predicted cNLSs, categorized per KPNA. The sequence of each candidate was submitted to the cNLS Mapper program with a cutoff score of 6. Candidates possessing a putative cNLS with a score of 6 or above (High) or below 6 (Low) were allocated to different categories. C. Pie chart of the subcellular localization of the identified proteins. The sequence of each candidate was assessed by PSORT II. Cyt, cytoplasm; nuc, nucleus; mit, mitochondria; end, endoplasmic reticulum; gol, Golgi body; pla, plasma membrane; pox, peroxisome; exc, extracellular.

reticulum, respectively. These results suggested that the subcellular localizations of the candidate KPNA7-binding proteins are similar to those of the KPNA2-binding proteins.

However, when the candidate binding proteins were subjected to Web-based functional analysis using the ToppGene software (https://toppgene.cchmc.org/) (Chen et al, 2009), the biological processes of the binding candidates of KPNA7 were quite different from those of KPNA2. Table 4 shows the top 10 most enriched GO biological processes for each KPNA. Interestingly, the KPNA7-binding proteins mainly had RNA-related functions such as (m)RNA processing, while KPNA2-interacting candidates were involved in a larger variety of biological processes.

Validation of candidate KPNA7- and KPNA2-binding proteins

Thirteen predicted candidate proteins were selected for validation; MSN, SORT1, CYFIP2, RAB3GAP2, RPTOR, AIFM1, CCNB1, DDB2, FANCI, KDM1A, PELO, TELO2, and PSME3. HEK293F cells were transfected with plasmids encoding the HA-tagged candidate proteins. EGFP-SV40T-NLS-GFP protein was used as a positive control. After 48 h of transfection, whole cell lysates were mixed with the GSH-immobilized GST-KPNA7 or GST-KPNA2 recombinant proteins. Bound proteins were detected by western blotting using anti-HA antibody. Of the tested proteins, SORT1, CYFI2, RPTOR, AIFM1, CCNB1, DDB2, FANCI,

Table 4. Web-based functional analysis of candidate proteins.

	ID	Name	p-value	Hit Count in Query List
KPNA7 binding proteins				
1	GO:0006396	RNA processing	2.81E-11	28
2	GO:0016071	mRNA metabolic process	1.46E-08	23
3	GO:0034660	ncRNA metabolic process	3.43E-08	16
4	GO:0006399	tRNA metabolic process	4.41E-08	11
5	GO:0046907	Intracellular transport	4.51E-07	33
6	GO:0016482	Cytoplasmic transport	5.78E-07	24
7	GO:0006397	mRNA processing	1.62E-06	16
8	GO:0043414	macromolecule methylation	4.73E-06	10
9	GO:0006370	7-methylguanosine mRNA capping	7.23E-06	5
10	GO:0006913	Nucleocytoplasmic transport	1.13E-05	14
KPNA2 binding proteins				
1	GO:0044403	Symbiosis, encompassing mutualism through parasitism	3.26E-08	20
2	GO:0044419	Interspecies interaction between organisms	3.26E-08	20
3	GO:0044764	Multi-organism cellular process	4.43E-08	19
4	GO:0006396	RNA processing	7.59E-08	19
5	GO:0016032	viral process	1.84E-07	18
6	GO:0034660	ncRNA metabolic process	8.88E-07	12
7	GO:0016482	Cytoplasmic transport	1.36E-06	19
8	GO:0016071	mRNA metabolic process	2.58E-06	16
9	GO:0006913	Nucleocytoplasmic transport	6.28E-06	12
10	GO:0051169	Nuclear transport	7.14E-06	12

KDM1A, PELO, and TELO2 more efficiently bound to GST-KPNA7 than to GST-KPNA2 (Figure 5). In contrast, PSME3 interacted more strongly with GST-KPNA2 than with GST-KPNA7. No binding with MSN and RAB3GAP2 was detected. These results suggested that SORT1, CYFIP2, RPTOR, AIFM1, CCNB1, DDB2, FANCI, KDM1A, PELO, and TELO2 can be transported to the nucleus in a KPNA7-dependent manner.

DDB2 is transported by KPNA7

To analyze the relation between KPNA7 and its candidate interaction partners further, I focused on DDB2, which showed a remarkable binding affinity for KPNA7 (Figure 5). Bacterially produced GFP-DDB2 protein was incubated with GSH-immobilized GST-KPNA7 and GST-KPNA2, and the bound protein was detected by western blotting using anti-GFP antibody (Figure 6A). As expected, GFP-DDB2 was effectively recognized by GST-KPNA7 and GST-KPNA2. In consistence with the result of the pull-down assay shown in Figure 5, KPNA7 interacted more effectively with DDB2 than with KPNA2. In addition, I conducted the pull-down assay using GST-GFP-DDB2 immobilized on GST beads with bacterially expressed GFP-KPNA7 and GFP-KPNA2 (Figure 6B). The results showed that the both KPNA proteins interacted with GST-GFP-DDB2, indicating that DDB2 binds directly to the KPNAs and that the binding affinity to KPNA7 is higher than that to KPNA2.

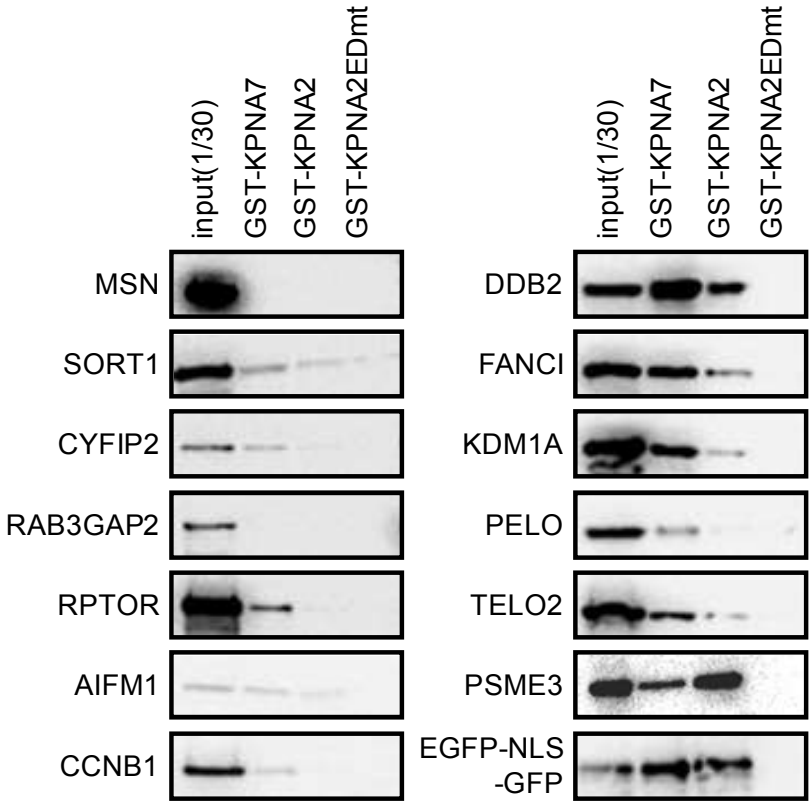

Figure 5. Validation analysis of KPNA7 or KPNA2.

Thirteen candidate proteins were tested for their capacity to bind full-length KPNA7 protein, KPNA2, or mutant KPNA2ED by GST pull-down assay. HA-tagged candidates were overexpressed in HEK293F cells and whole cell lysates were prepared after incubation for 48 h. SV40T-NLS-substrate (EGFP-NLS-GFP) was used as a positive control to bind to both importin αs. The lysates were incubated with GST-KPNA7, GST-KPNA2, or GST-KPNA2ED immobilized on GSH beads and bound proteins were analyzed by western blotting with anti-HA or anti-GFP.

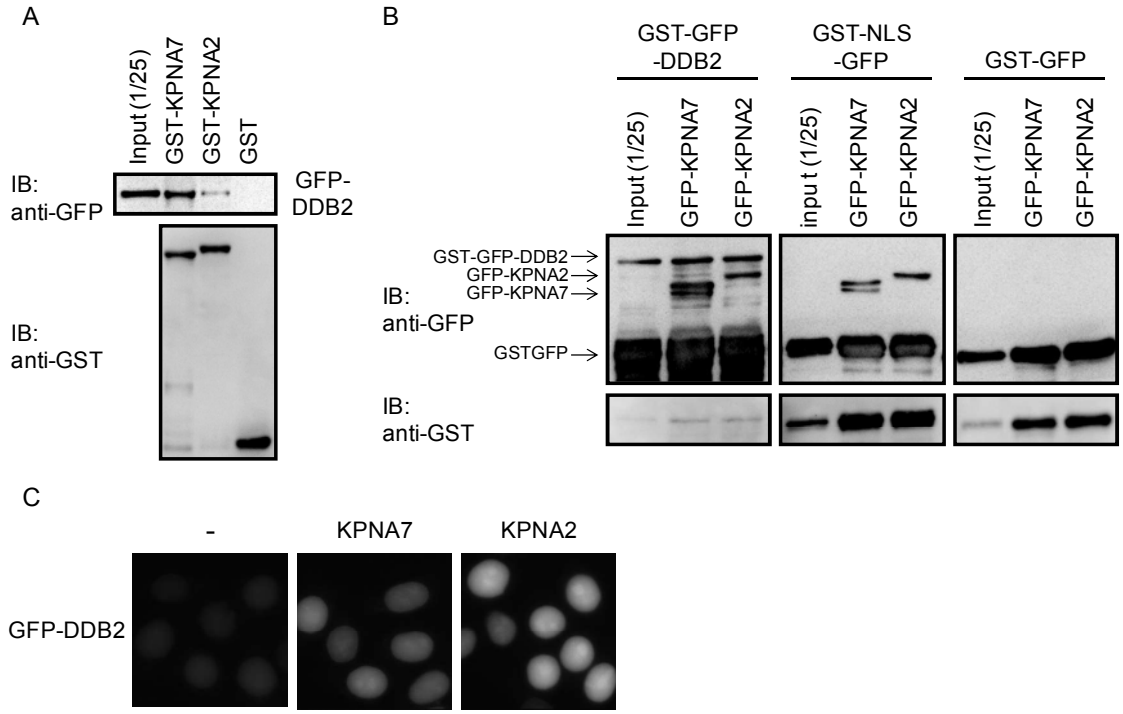

Figure 6. DDB2 is a cargo protein of KPNA7.

A. GST-KPNA7 and GST-KPNA2 (200 pmol each) were immobilized on GSH beads and incubated with GFP-DDB2 (200 pmol). Protein bands were detected with anti-GFP or anti-GST antibodies. B. GST-GFP-DDB2 (50 pmol) was immobilized on GSH beads and incubated with GFP-KPNA7 or GFP-KPNA2 (50 pmol each). Protein bands were detected with anti-GFP or anti-GST antibodies. GST-SV40TNLS-GFP and GST-GFP were used as a positive control or negative control, respectively. C. Digitonin-permeabilized HeLa cells were incubated with GFP-DDB2 or GST-SV40TNLS-GFP with importin β1, RanGDP, p10/NTF2, and an ATP regenerative system, with or without KPNA7 or KPNA2. After incubation for 30 min, the cells were observed under a fluorescence microscope.

Next, I performed an *in vitro* transport assay to test whether DDB2 is indeed imported into the nucleus by KPNA7 with importin β1. As shown in Figure 6C, GFP-DDB2 was obviously transported into the nucleus of HeLa cells in both the KPNA7- and KPNA2-dependent manner (Figure 6C), although the transport efficiency of KPNA7 was lower than that of KPNA2. Taken together, the results demonstrated that KPNA7 can bind directly to DDB2 and transport it into the nucleus via the classical importin α/β1 pathway, indicating that KPNA7 indeed functions as an NLS receptor.

KPNA7 forms heterodimers with other KPNAs, affecting their subcellular localization

The MS analysis indicated that KPNA3 is a KPNA7-binding protein. To know whether KPNA3 and KPNA4, which belong to the same subfamily, can bind to KPNA7, I performed a pull-down assay. HEK293F cells were transfected with plasmids encoding KPNA3 and KPNA4 fused to the 3xHA-tag. After 48 h of transfection, whole cell lysates were mixed with GST-KPNA7 and GST-KPNA2 recombinant proteins immobilized on GSH beads. Bound proteins were detected by western blotting using anti-HA antibody. Interestingly, both KPNA3 and KPNA4 strongly interacted with GST-KPNA7 (Figure 7A).

To date, there is no evidence of heterodimerization between KPNA family members and no knowledge on the putative physiological significance of heterodimerization on nuclear

transport. To address whether KPNA indeed forms heterodimers, I performed a GST pull-down assay. GST-KPNA7 and GST-KPNA2 were immobilized on GSH beads and incubated with FLAG-tagged KPNA1, KPNA2, and KPNA4. Interestingly, both GST-KPNA7 and GST-KPNA2 bound to all three FLAG-KPNA proteins (Figure 7B), although the homodimerization of KPNA2 was weak. There results indicated that KPNA7 as well as KPNA2 can form heterodimers with other KPNAs.

As shown in Figure 2D, EGFP-KPNA7 localized predominantly to the nucleus when it was overexpressed in HeLa cells, which was consistent with previously reported results obtained by using HA-KPNA7 (Kelley et al, 2010). In contrast, EGFP-KPNA2 was evenly distributed between the nucleus and cytoplasm, although it showed strong nuclear localization when highly expressed. Therefore, I examined the effect of KPNA7 expression on the subcellular localization of other importin α family members (Figure 8). Among the five tested importin αs, 3xHA-KPNA3 and 3xHA-KPNA4 were localized throughout the cells when expressed alone. In contrast, the nuclear localization of these two proteins was remarkably induced when the cells were co-transfected with KPNA7. The other KPNAs showed no significant changes in subcellular localization when co-expressed with KPNA7. From these findings, I hypothesize that KPNA7 is predominantly localized in the nucleus, where it can heterodimerize with other KPNAs such as KPNA3 and KPNA4, resulting

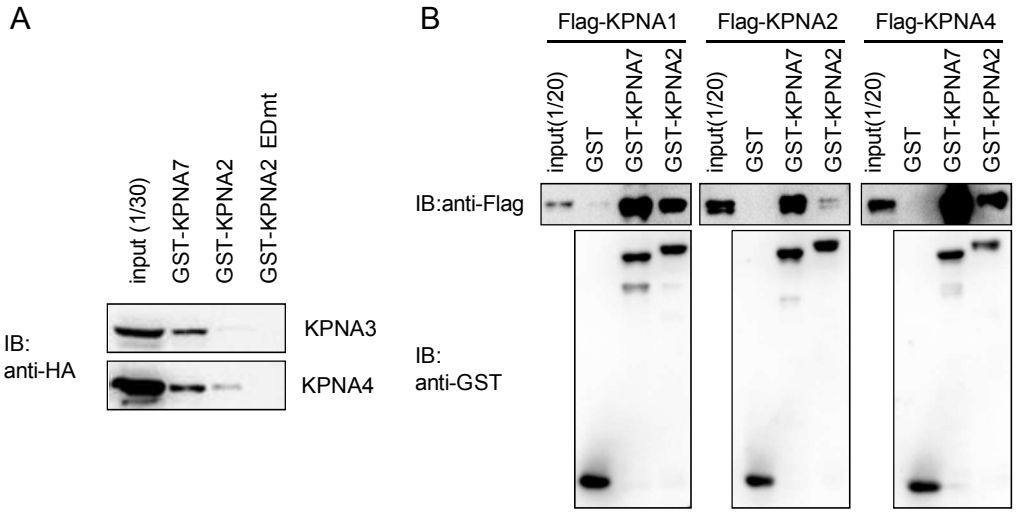

Figure 7. Interaction between KPNA7 and other KPNAs.

A. KPNA3 and KPNA4 were tested for their capacity to bind full-length KPNA7, full-length KPNA2, or mutant KPNA2ED by GST pull-down assay. HA-tagged KPNA3 and KPNA4 were overexpressed in HEK293F cells and whole cell lysates were prepared after incubation for 48 h. The lysate was incubated with GST-KPNA7, GST-KPNA2, or GST-KPNA2ED immobilized on GST beads, and bound proteins were analyzed by western blotting with anti-HA. B. GST-KPNA7 and GST-KPNA2 (200 pmol each) were immobilized on GSH beads and incubated with flag-KPNA1, flag-KPNA2, or flag-KPNA4 recombinant proteins (200 pmol). Bound proteins were detected by anti-FLAG or anti-GST antibody.

in the suppression of the recruitment of KPNAs to the cytoplasm and of the nuclear protein import.

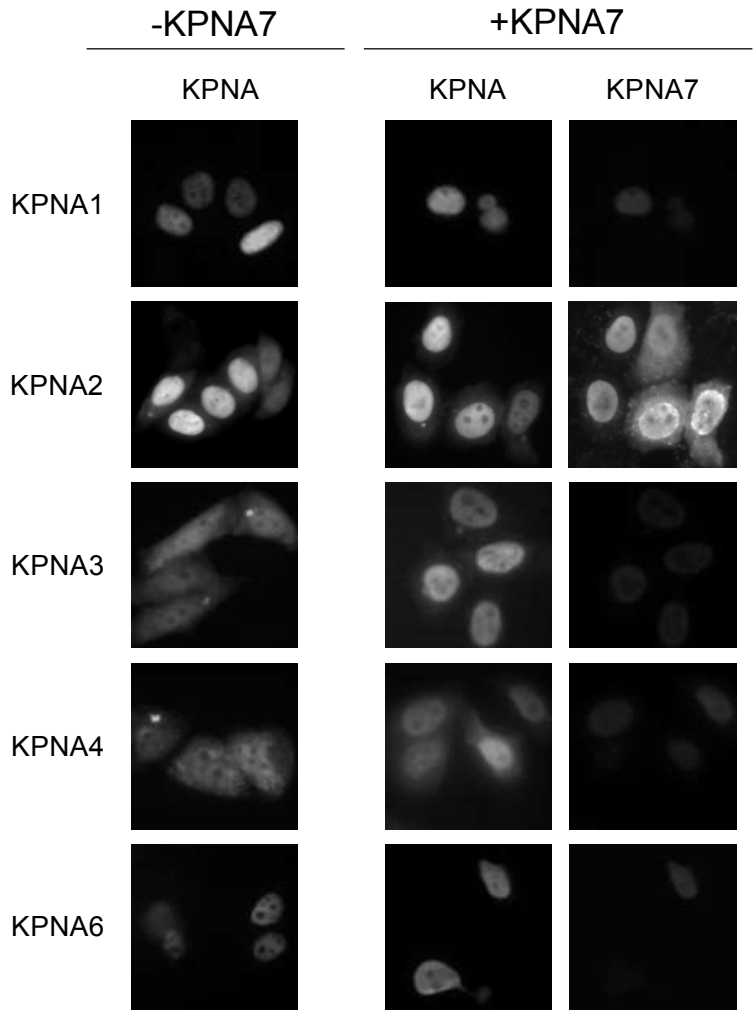

Figure 8. KPNA7 affects the subcellular localization of KPNA3 and KPNA4 in HeLa cell.

HeLa cells with or without 3xHA-KPNA7 plasmid were transfected with constructs encoding either 3xFLAG-tagged KPNA1 or KPNA6. HeLa cells with or without 3xFLAG-KPNA7 plasmid were transfected with constructs encoding 3xHA-tagged KPNA2, KPNA3, or KPNA4. After a 48-h incubation, the cells were fixed and immunostained with anti-HA and anti-FLAG.

DISCUSSION

This is the first study to show that KPNA7, in cooperation with importin β1, has nuclear transport ability. The amino acid similarity between hKPNA2 and hKPNA7 is quite low (53%), although they are categorized into the same subfamily. However, the amino acids in the major and minor NLS-binding sites that are critical for cNLS recognition are highly conserved between these two KPNAs. In consistence with this, like KPNA2, the KPNA7 protein interacted with the SV40T-NLS substrate and transported it into the nucleus. Furthermore, I demonstrated that KPNA7 transported DDB2, which was identified as one of the KPNA7-binding proteins, into the nucleus. These results indicated that KPNA7 is a functional cNLS receptor.

On the other hand, the subcellular distribution of KPNA7 and KPNA2 was clearly different; EGFP-KPNA7 was localized in the nucleus with strong nucleolar accumulation, while EGFP-KPNA2 was localized in both the nucleus and cytoplasm. The low amino acid similarity and differential subcellular localization may cause the variation in cargo proteins recognized by KPNA7 and KPNA2. Consistent with this, the pull-down assay and MS analysis exhibited that KPNA7 and KPNA2 have different interaction partners. In particular, a large fraction of the candidate KPNA7-binding proteins had RNA-related functions such as (m)RNA processing, which is a unique characteristic of KPNA7.

Both the MS analysis and the binding assay demonstrated that KPNA7 heterodimerizes with other KPNAs, particularly with KPNA3 and KPNA4. Moreover, cooexpression with KPNA7 resulted in a significant shift of the subcellular localization of KPNA3 and KPNA4 exogenously expressed in HeLa cells to the nucleus. *Xenopus leavis* importin α has been demonstrated to form homodimers and -multimers during purification (Görlich et al, 1994). In addition, it has recently been reported that KPNA2 can form an auto-inhibiting closed homodimer as shown by X-ray crystallography (Miyatake et al, 2014). While the physiological significance of multimerization of KPNAs has not been resolved until date, our data shed light on a novel regulation mechanism in KPNA-mediated classical nuclear transport; By retaining KPNA3 and KPNA4 in the nucleus, KPNA7 may suppress the nuclear import of distinct KPNA-specific cargoes such as NF-κB (Fagerlund et al, 2005) and STAT3 (Liu et al, 2005) (depicted as cargo protein "A" in Figure 9B, C). However, KPNA7 has the ability to transport cNLS-containing proteins into the nucleus in concerted action with importin β1, as I demonstrated in this study (Figure 9A).

It has been demonstrated in our laboratory that the KPNA family proteins can have opposite functions as "import driver" or "import suppressor." While Snail, a zinc finger-containing transcription factor, is transported into the nucleus by importin β1, KPNA1 competes with importin β1 for zinc finger domain-binding, resulting in reduced nuclear import

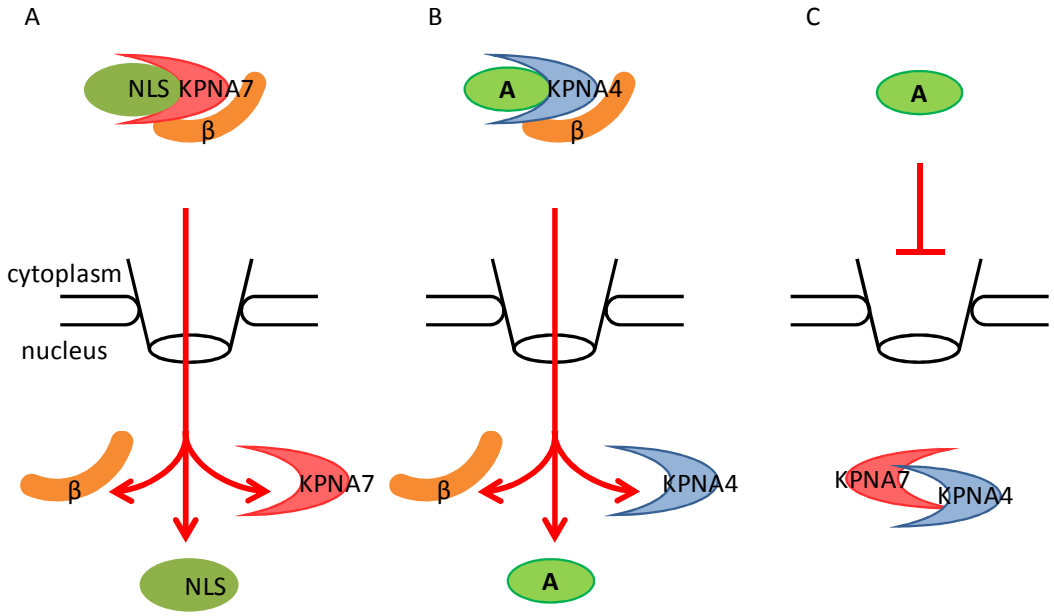

Figure 9. A KPNA7 functional model.

A. KPNA7 can transport a cNLS-containing cargo protein (indicated as NLS) from the cytoplasm to the nucleus with importin β1 (β). B. KPNA4 can transport the cargo protein (A) from the cytoplasm to the nucleus with importin β1. C. KPNA7 binds to KPNA4 to form a heterodimer in the nucleus, which may inhibit the nuclear transport of KPNA4-specific cargo.

of Snail (Sekimoto et al, 2011). In addition, a short acidic stretch in the C-terminus of KPNA2, which was recently identified as a binding site for the neural lineage transcription factor Oct6, mediates cytoplasmic retention of Oct6 in undifferentiated ES cells (Yasuhara et al, 2013). Therefore, I speculate that KPNA heterodimer formation by KPNA7, causing the retention of other KPNAs in the nucleus, is a third mode of negative regulation in classical nuclear transport. The highly specific expression of KPNA7 in oocytes (Tejomurtula et al, 2009) and pancreatic cancer cell lines (Laurila et al, 2014) suggests that the negative regulation occurs only in specific cells. It will be interesting to know how the heterodimerization affects the nuclear transport of distinct cargos in living cells.

It has been reported that abnormal function of KPNA7 is associated with severe diseases. KPNA7 promotes malignant properties of pancreatic cancer (Laurila et al, 2014). This report demonstrated that KPNA7 is not only expressed in oocytes, but also in pancreatic cancer cells. In addition, the two amino acid substitutions (P399A, E345Q) in hKPNA7 are known to cause infantile spasms and cerebellar malformation (Paciorkowski et al, 2014). Because KPNA7 is a putative regulator of nuclear transport as revealed in this study, it will be interesting to understand the specific roles of KPNA7 in the pathogenesis of various diseases.

Although KPNA7 has been classified into the KPNA2 subfamily based on the amino acid sequence similarity, the similarity is only 55%, which is lower than that within other

subfamilies. In addition, it has been shown that KPNAs belonging to the same subfamily show similar substrate-specificity. The proteomics analysis revealed that only 62 out of 250 candidate interacting proteins were common between KPNA2 and KPNA7. These results suggested that both proteins have distinct substrate specificities. Moreover, I found that the subcellular localization of KPNA7 is different from that of KPNA2 (Figure 2D), consistent with previously reported results (Kelley et al, 2010). Based on all the results and taking into account the dimerization properties of KPNA7, I propose that KPNA7 should be classified into a new subfamily apart from KPNA2, and thus that KPNAs should be divided into four, rather than three classes (Figure 10).

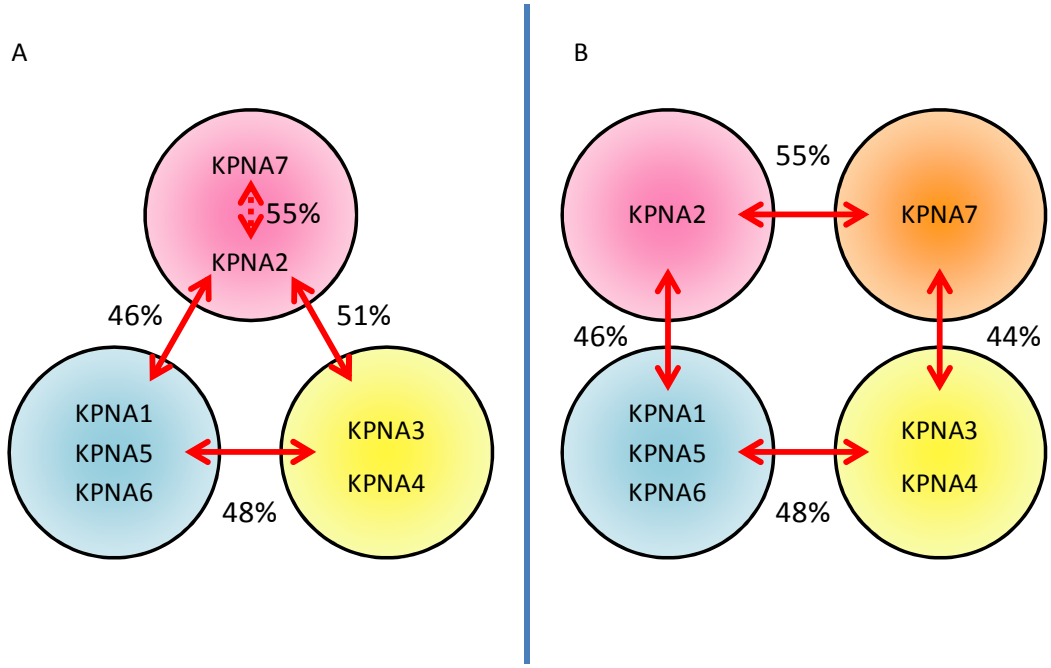

Figure 10. KPNA7 can be classified into the fourth subfamily of KPNAs.

A. KPNAs are traditionally classified into three subfamilies. B. KPNAs can be classified into four subfamilies, based on the evidence obtained in this study that KPNA7 belongs to another subfamily than KPNA2.

ACKNOWLEDGEMENTS

My heartfelt appreciation goes to Dr. Yoshihiro Yoneda who provided accurate advice. I would like to express my gratitude to Dr. Masahiro Oka and Dr. Yoichi Miyamoto whose knowledge, insights, and academic experience have been of invaluable help to me. I am also extremely grateful to members of the laboratory. Dr. Noriko Yasuhara and Dr. Tetsuji Moriyama offered their unreserved help and guidance and led me to perform my research systematically. Ms. Hitomi Inoue gave me technical support. Dr. Koji Yamada, Dr. Akira Tsujii, Mr. Shu Tanaka, and Ms. Masako Harayama supported me in the laboratory. I also thank Professor Chikashi Obuse for the mass spectrometry analysis and Dr. Yoshinobu Igarashi for the web-based bioinformatics analysis of importin α-binding candidates. I would also like to express my gratitude to my family for their moral support and warm encouragement.

REFERENCES

Arjomand A, Baker MA, Li C, Buckle AM, Jans DA, Loveland KL, Miyamoto Y (2014) The alpha-importome of mammalian germ cell maturation provides novel insights for importin biology. *FASEB J* **28:** 3480-3493

Chen J, Bardes EE, Aronow BJ, Jegga AG (2009) ToppGene Suite for gene list enrichment analysis and candidate gene prioritization. *Nucleic Acids Res* **37:** W305-311

Cronshaw JM, Krutchinsky AN, Zhang W, Chait BT, Matunis MJ (2002) Proteomic analysis of the mammalian nuclear pore complex. *J Cell Biol* **158:** 915-927.

Fontes MR, Teh T, Kobe B (2000) Structural basis of recognition of monopartite and bipartite nuclear localization sequences by mammalian importin-alpha. *Journal of Molecular Biology* **297:** 1183-1194

Fagerlund R, Kinnunen L, Kohler M, Julkunen I, Mele´n K (2005) NF-κB is transported into the nucleus by Importin α3 and Importin α4. **280:** 15942–15951

Goldfarb DS, Corbett AH, Mason DA, Harreman MT, Adam SA (2004) Importin α: a multipurpose nuclear-transport receptor. *Trends Cell Biol* **14:** 505-514

Görlich D, Prehn S, Laskey RA, Hartmann E. (1994) Isolation of a protein that is essential for the first step of nuclear protein import. *Cell* **79:** 767-778

Hoelz A, Debler EW, Blobel G (2011) The structure of the nuclear pore complex. *Annu Rev Biochem* **80:** 613-643

Hu J, Wang F, Yuan Y, Zhu X, Wang Y, Zhang Y, Kou Z, Wang S, Gao S (2010) Novel importin-alpha family member Kpna7 is required for normal fertility and fecundity in the mouse. *J Biol Chem* **285:** 33113-33122

Kelley JB, Talley AM, Spencer A, Gioeli D, Paschal BM (2010) Karyopherin alpha7 (KPNA7), a divergent member of the importin alpha family of nuclear import receptors. *BMC Cell Biol* **11:** 63

Kobe B (1999) Autoinhibition by an internal nuclear localization signal revealed by the crystal structure of mammalian importin α. *Nature structural biology* **6:** 388-397

Kohler M, Ansieau S, Prehn S, Leutz A, Haller H, Hartmann E (1997) Cloning of two novel human importin-alpha subunits and analysis of the expression pattern of the importin-alpha protein family. *FEBS Lett* **417:** 104-108

Kohler M, Speck C, Christiansen M, Bischoff FR, Prehn S, Haller H, Gorlich D, Hartmann E (1999) Evidence for distinct substrate specificities of importin alpha family members in nuclear protein import. *Mol Cell Biol* **19:** 7782-7791

Kosugi S, Hasebe M, Tomita M, Yanagawa H (2009) Systematic identification of cell cycle-dependent yeast nucleocytoplasmic shuttling proteins by prediction of composite motifs. *Proc Natl Acad Sci U S A* **106:** 10171-10176

Laurila E, Vuorinen E, Savinainen K, Rauhala H, Kallioniemi A (2014) KPNA7, a nuclear transport receptor, promotes malignant properties of pancreatic cancer cells in vitro. *Exp Cell Res* **322:** 159-167

Liu L, McBride KM, Reich NC (2005) STAT3 nuclear import is independent of tyrosine phosphorylation and mediated by importin-alpha3. *Proc Natl Acad Sci U S A.* **102:**8150-5.

Madrid AS, Weis K (2006) Nuclear transport is becoming crystal clear. *Chromosoma* **115:** 98-109

Mason DA, Fleming RJ, Goldfarb DS (2002) Drosophia melanogaster importin alpha 1 and alpha 3 can replace importin alpha 2 during spematogenesis but not oogenesis. *Genetics* **161:** 157-70

Mason DA, Mathe E, Fleming RJ, Goldfarb DS (2003) The Drosophila melanogaster importin alpha3 locus encodes an essential gene required for the development of both larval and adult tissues. *Genetics* **165:** 1943-58

Miyamoto Y, Baker MA, Whiley PA, Arjomand A, Ludeman J, Wong C, Jans DA, Loveland KL (2013) Towards delineation of a developmental α-importome in the mammalian male germline. *Biochim Biophys Acta* **1833:** 731-742

Miyamoto Y, Boag PR, Hime GR, Loveland KL (2012) Regulated nucleocytoplasmic transport during gametogenesis. *Biochim Biophys Acta* **1819:** 616-630

Miyamoto Y, Imamoto N, Sekimoto T, Tachibana T, Seki T, Tada S, Enomoto T, Yoneda Y (1997) Differential modes of nuclear localization signal (NLS) recognition by three distinct classes of NLS receptors. *J Biol Chem* **272:** 26375-26381

Miyatake H, Sanjoh A, Unzai S, Matsuda G, Tatsumi Y, Miyamoto Y, Dohmae N, Aida Y (2014) Crystal structure of human importin-α1 (Rch1): A novel autoinhibition mechanism by homodimerization. *PloS ONE* in press

Moriyama T, Nagai M, Oka M, Ikawa M, Okabe M, Yoneda Y (2011) Targeted disruption of one of the importin a family members leads to female functional incompetence in delivery. *FEBS J* **278:** 1561-72

Nakai K, Horton P (1999) PSORT: a program for detecting sorting signals in proteins and predicting their subcellular localization. *Trends Biochem Sci* **24:** 34-36

Nozawa RS, Nagao K, Masuda HT, Iwasaki O, Hirota T, Nozaki N, Kimura H, Obuse C (2010) Human POGZ modulates dissociation of HP1alpha from mitotic chromosome arms through Aurora B activation. *Nat Cell Biol* **12:** 719-27

Paciorkowski AR, Weisenberg J, Kelley JB, Spencer A, Tuttle E, Ghoneim D, Thio LL, Christian SL, Dobyns WB, Paschal BM (2014) Autosomal recessive mutations in nuclear transport factor KPNA7 are associated with infantile spasms and cerebellar malformation. *European journal of human genetics : EJHG* **22:** 587-593

Park KE, Inerowicz HD, Wang X, Li Y, Koser S, Cabot RA (2012) Identification of karyopherin alpha1 and alpha7 interacting proteins in porcine tissue. *PLoS One* **7:** e38990

Ratan R, Mason DA, Sinnot B, Goldfarb DS, Fleming RJ (2008) Drosophia importin alpha1 preforms paralog-specific functions essential for gametogenesis. *Genetics* **178:** 839-50

Rout MP, Aitchison JD, Suprapto A, Hjertaas K, Zhao Y, Chait BT (2000) The yeast nuclear pore complex: composition, architecture, and transport mechanism. *J Cell Biol* 148**:** 635-651

Sekimoto T, Imamoto N, Nakajima K, Hirano T, Yoneda Y (1997) Extracellular signal-dependent nuclear import of Stat1 is mediated by nuclear pore-targeting complex formation with NPI-1, but not Rch1. *EMBO J* **16:** 7067-7077

Sekimoto T, Miyamoto Y, Arai S, Yoneda Y (2011) Importin alpha protein acts as a negative regulator for snail protein nuclear import. *J Biol Chem* **286:** 15126-31

Sorokin AV, Kim ER, Ovchinnikov LP (2007) Nucleocytoplasmic transport of proteins. *Biochemistry (Mosc)* **72:** 1439-1457

Tejomurtula J, Lee KB, Tripurani SK, Smith GW, Yao J (2009) Role of importin alpha8, a new member of the importin alpha family of nuclear transport proteins, in early embryonic development in cattle. *Biol Reprod* **81:** 333-342

Tsuji L, Takumi T, Imamoto N, Yoneda Y (1997) Identification of novel homologues of mouse importin α, the alpha subunit of the nuclear pore-targeting complex, and their tissue-specific expression. *FEBS Lett* **416:** 30-34

Wente SR, Rout MP (2010) The nuclear pore complex and nuclear transport. *Cold Spring Harb Perspect Biol* **2:** a000562

Yasuhara N, Yamagishi R, Arai Y, Mehmood R, Kimoto C, Fujita T, Touma K, Kaneko A, Kamikawa Y, Moriyama T, Yanagida T, Kaneko H, Yoneda Y (2013) Importin alpha subtypes determine differential transcription factor localization in embryonic stem cells maintenance. *Dev Cell* **26:** 123-135

Yokoya F, Imamoto N, Tachibana T, Yoneda Y (1999) beta-catenin can be transported into the nucleus in a Ran-unassisted manner. *Mol Biol Cell* **10:** 1119-1131

PUBLICATIONS AND PRESENTATIONS

Publications

○Moriya K, Yamamoto T, Takamitsu E, Matsunaga Y, Kimoto M, Fukushige D, Kimoto C, Suzuki T, Utsumi T (2012) Protein N-myristoylation is required for cellular morphological changes induced by two formin family proteins, FMNL2 and FMNL3. *Biosci Biothechnol Biochem* **76:** 1201-9

○Yasuhara N, Yamagishi R, Arai Y, Mehmood R, Kimoto C, Fujita T, Touma K, Kaneko A, Kamikawa Y, Moriyama T, Yanagida T, Kaneko H, Yoneda Y (2013) Importin alpha subtypes determine differential transcription factor localization in embryonic stem cells maintenance. *Dev Cell* **26:** 123-35

Presentations

○第 63 回日本細胞生物学会大会(2011)

NLS 配列による核輸送経路決定のメカニズム

Chihiro Kimoto, Noriko Yasuhara, Yoshihiro Yoneda

○第 84 回日本生化学大会(2011)

NLS による核輸送経路決定のメカニズム

Chihiro Kimoto, Noriko Yasuhara, Yoshihiro Yoneda

○第 10 回核ダイナミクス研究会(2011)

POU family における NLS による核輸送経路決定のメカニズム

Chihiro Kimoto, Noriko Yasuhara, Yoshihiro Yoneda

○第 34 回日本分子生物学会年会(2011)

The mechanism to determine a nuclear transport pathway by NLS sequence.

Chihiro Kimoto, Noriko Yasuhara, Yoshihiro Yoneda

○第 45 回日本発生生物学会・第 64 回日本細胞生物学会合同大会(2012)

Recognition mode of basic NLS sequence by importin α1.

Chihiro Kimoto, Noriko Yasuhara, Yoshihiro Yoneda

○第 35 回日本分子生物学会年会(2012)

Recognition pattern of basic NLS sequence by importin α1.

Chihiro Kimoto, Noriko Yasuhara, Yoshihiro Yoneda

○第 30 回染色体 WS・第 11 回核ダイナミクス研究会合同開催

Importin α1 による塩基性核局在化シグナル配列認識の様式

Chihiro Kimoto, Noriko Yasuhara, Yoshihiro Yoneda